RESPONSE OF A UNIFORM FREE-PINNED BEAM TO LATERAL SINUSOIDAL AND RANDOM EXCITATION

Thesis by

Theodore E. Lang

In Partial Fulfillment of the Requirements

For the Degree of

Mechanical Engineer

California Institute of Technology

Pasadena, California

1961

ACKNOWLEDGEMENT

The author wishes to express his appreciation to the members of his committee for their helpful advice and comments during the course of this research.

ABSTRACT

The equation of motion for a beam in flexure is solved for a free-pinned beam excited by two types of point forcing functions. The two forcing functions, one varying sinusoidally in time and the other randomly, are expressed in terms of a displacement input at the pinned end of the beam. The response of the beam is expressed in terms of strain as a function of location along the length of the beam.

The results of an experiment to evaluate the damping coefficient for each of the five lowest bending modes of the beam are reported. The damping coefficients were calculated from the equation for the response of the beam to sinusoidal excitation using experimentally measured values of the displacement at the input end and strain along the beam.

TABLE OF CONTENTS

PART	TITLE	PAGE
	Acknowledgements	
	Abstract	
	List of Figures	
	List of Tables	
	Notation	
I.	Introduction	1
II.	Review of Beam Theory	
	A. Solution of the Bernoulli-Euler Beam Equation for a Free-Pinned Beam Excited by a Sinusoidal Displacement at the Pinned End	5
	B. Derivation of the Response Equation for a Free-Pinned Beam Excited by a Random Displacement at the pinned End	15
	1. Bandwidth of Excitation Frequencies: $0<\omega<\infty$	15
	2. Bandwidth of Excitation Frequencies: $0<\omega<\omega_c$	20
III.	Experimental Determination of Damping	
	A. Apparatus	29
	B. Testing Procedure	33
	C. Evaluation of Experimental Data	36
	D. Discussion of Results	44
	Appendix A: Calculation of the Calibration Strain Value	51
	Appendix B: Evaluation of the Integral $\int_0^l x\, \Phi_n(\beta_n x)\, dx$	54
	List of References	55

LIST OF FIGURES

FIGURE NO.	TITLE	PAGE
I.	Diagram of the free-pinned beam.	5
II.	Diagram of the free-pinned beam showing the force F(t) producing the displacement D(ℓ) at the pinned end.	11
III.	Example of a clipped spectrum of mean squared acceleration.	21
IV.	Plot of the clipping correction factor (R_{cn}) verses the frequency ratio (ω_c/ω_n).	25
V.	Diagram of the test bar and its supports.	30
VI.	Strain gage bridge circuit.	32
VII.	Schematic diagram of the equipment setup for the sinusoidal vibration tests.	34
VIII.	Plot of the experimental damping coefficients (λ_n) verses the normal mode frequencies for the five lowest bending modes of the beam.	40
IX.	Plot of the fraction of critical damping (c/c_c) verses the normal mode frequencies for the five lowest bending modes of the free-pinned beam.	42
X.	Calculated and experimental response curves for the first bending mode at station x/ℓ = 0.772.	45
XI.	Calculated and experimental response curves for the second bending mode at station x/ℓ = 0.772.	46
XII.	Calculated and experimental response curves for the third bending mode at station x/ℓ = 0.772.	47
XIII.	Strain gage calibration circuit.	51

LIST OF TABLES

TABLE NO.	TITLE	PAGE
I.	Values of the parameters for the five lowest bending modes of the free-pinned test beam.	38
II.	Average experimental values of the damping coefficients for the five lowest beam bending modes.	39
III.	Summary of test data.	43

NOTATION

ROMAN LETTERS

a	Constant (see equation 51)
a_n	Constant (defined on page 22)
A	Cross sectional area of beam (in.^{2})
b_m, b_n	Constants (see equation 52)
c	Half thickness of beam (in.)
C_{in}	i^{th} constant of normal function (see equation 8)
D_o	Rigid body displacement amplitude (see equation 23)
$D(x), D(x')$	Rigid body deflection (in.)
Δe	Voltage unbalance of strain gage bridge (volts)
E	Modulus of elasticity (lb./in.^{2})
$f(t)$	Time variation of forcing function
f, f_n	Frequency (cps)
$F(t)$	Forcing function (lb.)
F_o	Magnitude of forcing function (lb.)
G	Acceleration spectral density $\left[\frac{(\text{in./sec.}^2)^2}{\text{cps}}\right]$
$h(t)$	Unit impulse response
H	Linear time differential operator (see equation 14)
i	Subscript, also $\sqrt{-1}$
I	Mass moment of inertia of beam (lb.-sec.^{2}-in.)
I_z	Moment of inertia of beam cross-section about the z axis (in.^{4})
J	Integral (defined in Appendix B, page 54)
K	Strain gage factor (see equation A-9, Appendix A)
l	Length of beam (in.)

NOTATION (CONTD.)

ROMAN LETTERS

m	Subscript denoting mode number
M	Mass of beam $\left[\frac{\text{lb.-sec.}^2}{\text{in.}}\right]$
M_1	Bending moment [in.-lb.]
n	Subscript denoting mode number
$P_n(t)$	Forcing function
$\mathcal{P}_n(t)$	Generalized forcing function
Q	Resonant amplification factor
$Q_n(t)$	Generalized forcing function
$\eta_n(t)$	Independent variable
R_1, R_2, R_3, R_4	Strain gage resistances (ohm)
R_c	Calibration resistor (ohm)
R_{cn}	Clipping correction factor (see equation 68)
t	Time (sec.)
$u, u(t)$	Total transverse displacement of beam (in.)
u_e	Elastic transverse deformation of beam (in.)
$\overline{u_{e_n}^2}$	Mean squared displacement of the n^{th} mode (in.2)
u_n	Rigid body displacement of beam (in.)
V	Battery voltage to strain gage bridge (volts)
x, x'	Rectangular coordinate along longitudinal axis of beam
y, y'	Rectangular coordinate normal to bending plane of beam
Y	Lateral displacement (in.)
Y_o	Maximum rigid body displacement (in.)
z, z'	Rectangular coordinate normal to the other axes defined above

NOTATION (CONTD.)

ROMAN LETTERS

$\mathcal{Z}$	Substitute variable
Z	Impedance function

GREEK LETTERS

α	Exponent in damping coefficient (see equation 75)
α_n	Beam parameter for the n^{th} mode (see equation 12)
β_n	Beam parameter for the n^{th} mode (see equation 7)
γ	Constant (see equation 69)
$\delta(t), \delta(t-\tau)$	Dirac Delta Function
ϵ	Extensional Strain (in./in.)
$\mathcal{I}_n$	Beam parameter for the n^{th} mode (see equation 32)
$\eta_n(t)$	Generalized time variable (sec.)
θ	Angle of rigid body rotation (rad.)
θ_0	Maximum angle of rigid body rotation (rad.)
θ_1, θ_2	Phase angles (see equations 53 and 54)
λ_n	Damping coefficient for the n^{th} mode ($sec.^{-1}$)
μ	Constant in damping coefficient (see equation 75)
ν	Strain rate coefficient (see Discussion of Results on page 44)
ξ	Constant (see equation 70)
ρ	Density $\left[\frac{(lb.\text{-}sec.^2)}{in.^4}\right]$
$\sigma, \sigma(y)$	Normal bending stress ($lb./in.^2$)
τ, τ'	Time (sec.)
ϕ_n	Phase angle (see equation 39)

NOTATION (CONTD.)

GREEK LETTERS

$\Phi_n, \Phi_n(\beta_n x)$	Normal function (see equation 11)
$\Phi(\omega)$	Acceleration spectral density $\left[\frac{(\text{in./sec.}^2)^2}{\text{rad/sec}}\right]$
$\Psi_n, \Psi_n(\beta_n x)$	Beam parameter (see equation 42a on page 36)
$\omega, \omega_c, \omega_n$	Frequency (sec.^{-1})

I. INTRODUCTION

When a system is driven by an excitation that is random in time, the phase and periodicity are no longer important since the instantaneous response is not predictable. Instead one may attempt to determine the statistical properties of the excitation and define the mean squared response of the system. The statistical description and techniques of using random variables in analyses are due primarily to Rice (1) and Weiner (2). In the last decade these concepts have been applied extensively to analyze problems in communication, structural design, fatigue and earthquakes.

In the field of aircraft and missile structural dynamics, Liepmann (3) solved the one dimensional problem of buffeting of airfoils due to air turbulence. Later Miles (4) considered the problem of panel vibration due to jet noise. In these analyses the panel or airfoil was represented as a single degree-of-freedom system in which the forcing function was random in time but spacewise constant. Later Lassiter, Hess and Hubbard (5) experimentally verified Miles' theory for the mean square response of thin panels when excited by jet noise.

Spacial as well as time variations may occur in random excitation of beams and plates. Some of the theoretical work in this field was done by Thomson and Barton (6), Eringen (7), and Samuels and Eringen (8). Thomson and Barton outlined a solution for the response of a free-free beam to random excitation and represented the forcing function by an acceleration spectral density. Eringen, using a generalized harmonic analysis developed by Weiner (9), derived expressions for the damped beam and plate response in terms of cross correlation functions of the

displacements, moments and stresses. Later Samuels and Eringen extended this method to the Timoshenko beam theory which includes shear deformation and rotary inertia. More recently Stumpf (10) has summarized and illustrated many of the basic principles in random vibration analysis including a discussion of three approaches to solving random excitation problems, depending upon the information known about the input.

The calculation of the response of a beam to a random forcing function is dependent upon knowledge of certain of the beam properties and parameters. For sinusoidal excitation of a uniform beam, specification of the size, material and end constraints is sufficient information to calculate the beam response except at resonance, where the calculated response is infinite unless a damping term is included in the equation of motion. When the beam is excited randomly, the response is expressed in terms of mean squared values of displacement, stress, etc., and the major contribution to these quantities is from the resonant and near resonant amplitudes of the beam. Therefore, in deriving the response equation for a beam excited randomly, it is essential to approximate or evaluate the damping in the beam and include a damping term in the equation of motion in order to avoid obtaining an infinite value for the calculated response.

The motion of a beam when the excitation is random can be expressed analytically by a superposition of normal modes, as in the case of sinusoidal excitation. However, because the response is made up of a distribution of normal modes, it generally is necessary to know the damping in several modes of the beam in order to calculate the approximate total response. The number of modes for which the damping

must be evaluated is a function of the exact nature of the random forcing function and the rapidity of convergence of the response equation with mode number. Many techniques and methods have been devised for measuring damping in materials and structures, and the subject is widely discussed in the literature. For a comprehensive summary of the more common methods of measuring damping, reference is made to Section 5 of the book "Structural Damping" edited by J. E. Ruzicka (11).

A convenient method of measuring the damping in several normal modes of a beam utilizes the response at resonance of each normal mode as determined experimentally. Measurement is made of the amplitude of the sinusoidal excitation and output; then, using derived equations that include an arbitrary damping term, the damping term is evaluated in the modes for which data are taken. This method for measuring damping is similar to the method used with simple oscillators in which the resonant amplification factor is measured and then related to the viscous damping coefficient (c/c_c), [Reference (11)]. The details of introducing an arbitrary damping term in the equation of motion of a beam is discussed in more detail in the text of this thesis.

Therefore, the objectives of the work reported in this thesis were first, to review the theoretical aspects of the beam problem by solving the forced motion equation for a free-pinned beam in which there was included a damping term related to the hysteresis properties of the beam material. The forcing function acting on the beam was represented by a lateral displacement of the pinned end, and solutions were derived for both sinusoidal and random time-variations of this force. The second objective was to determine experimentally the values of the

damping coefficients for the five lowest bending modes of a test beam that was supported with "free-pinned" end constraints. The damping coefficients for each mode were calculated from the response of the beam at its resonances.

II. REVIEW OF BEAM THEORY

A. SOLUTION OF THE BERNOULLI-EULER BEAM EQUATION FOR A FREE-PINNED BEAM EXCITED BY A SINUSOIDAL DISPLACEMENT AT THE PINNED END

Consider a beam with a free end at $x = 0$ and a pinned end at $x = \ell$, driven at the pinned end by a time varying displacement $u(t)$ (Figure I).

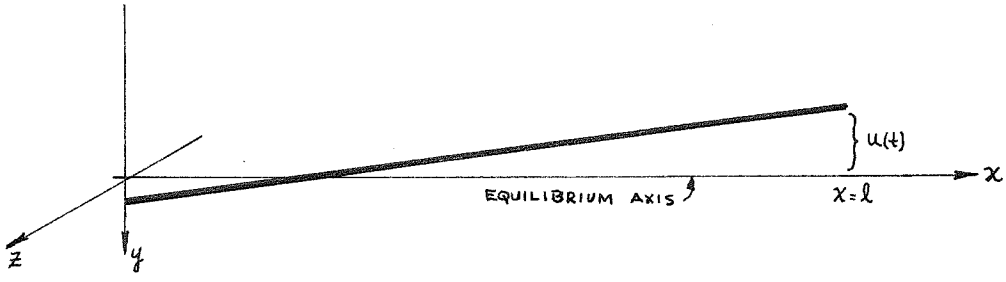

Figure I: Diagram of the free-pinned beam showing the rigid body displacement $u(t)$ at the pinned end, and the orientation of the coordinate axes x, y and z with origin at the free end.

The Bernoulli-Euler beam equation [Reference (12)] is:

$$EI_z \frac{\partial^4 u}{\partial x^4} + \rho A \frac{\partial^2 u}{\partial t^2} = 0 \qquad (1)$$

We assume that the lateral displacement of the beam at any point along its length is the summation of two parts, one part being the rigid body displacement (u_r) and the other part being the flexural deformation of the beam (u_e):

$$u = u_r + u_e \qquad (2)$$

Substitution of equation 2 into equation 1 results in the following:

$$EI_z \frac{\partial^4 u_e}{\partial x^4} + \rho A \frac{\partial^2 u_e}{\partial t^2} = -\rho A D(x) \ddot{f}(t) \qquad (3)$$

where the substitution was made that $u_r = D(x) f(t)$. Because there is no curvature change (bending) associated with the rigid body motion

of the beam, the rigid body displacement D(x) is of lower than fourth order in x. Hence, the rigid body displacement contributes only to the inertia loading on the beam.

The normal function and frequency equation are determined from the homogeneous part of equation 3, namely:

$$\frac{\partial^4 u_e}{\partial x^4} + \frac{\rho A}{E I_z} \frac{\partial^2 u_e}{\partial t^2} = 0 \tag{4}$$

Using separation of variables, a solution to equation 4 is

$$u_e = \sum_{n=1}^{\infty} \Phi_n(x)\, e^{i\omega t} \tag{5}$$

The function $\Phi_n(x)$ must satisfy the following differential equation:

$$\frac{d^4 \Phi_n}{dx^4} - \beta_n^4 \Phi_n = 0 \tag{6}$$

where

$$\beta_n^4 = \frac{\rho A \omega_n^2}{E I_z} \tag{7}$$

The general solution to equation 6 is

$$\Phi_n(\beta_n x) = C_{1n} \sin \beta_n x + C_{2n} \cos \beta_n x + C_{3n} \sinh \beta_n x + C_{4n} \cosh \beta_n x \tag{8}$$

The constants in equation 8 must be defined such that the equation satisfies the boundary conditions. The boundary conditions are:

$$\frac{d^2 \Phi_n}{dx^2} = 0 \quad , \quad \frac{d^3 \Phi_n}{dx^3} = 0 \qquad \text{at the free end } (x = 0) \tag{9}$$

and

$$\Phi_n = 0 \quad , \quad \frac{d^2 \Phi_n}{dx^2} = 0 \qquad \text{at the pinned end } (x = \ell) \tag{10}$$

Three of the constants in equation 8 can be defined in terms of the

fourth by application of equations 9 and 10. The result is

$$\Phi_n(\beta_n x) = C_{1n}\left[\cos\beta_n x + \cosh\beta_n x - \alpha_n\left[\sin\beta_n x + \sinh\beta_n x\right]\right] \tag{11}$$

where

$$\alpha_n = \frac{\cos\beta_n l + \cosh\beta_n l}{\sin\beta_n l + \sinh\beta_n l} \tag{12}$$

The constant C_{1n}, although it does not appear in the final solution, is defined such that the value of the orthogonality integral in the denominator of the generalized forcing function (equation 22) is a simple multiple of the beam length. Finally, the frequency equation is

$$\tan\beta_n l = \tanh\beta_n l \tag{13}$$

In order to represent analytically the resonant and near resonant response of the beam to a forcing function, it is necessary to include a damping term in the equation of motion. The type of damping depends upon the mechanism by which the beam dissipates energy; in general, the particular types of dissipation or damping can be determined only by experiment. However, for purposes of analysis, the category of dissipation characteristics can be defined generally. For example, if the excitation is at relatively low frequencies and at low amplitudes, damping due to the surrounding air is probably negligible compared to internal or hysteresis type damping. In addition, if structural connections are made rigid, damping due to sliding friction is also unimportant. In the following analysis we shall use a mathematical representation of damping that relates to the hereditary stress-strain law of the material (hysteresis type damping).

The effect of damping is introduced into the analysis by including in the differential equation for the beam, equation 3, an additional term which includes a stress increment dependent upon the rate of strain. In effect, such stress increment accounts for the hysteresis damping. The form of the function is left undefined in recognition of the fact that the mechanism of hysteresis damping is not well understood. However, the effect of the damping on the response of the beam in each normal mode is described by evaluating experimentally a frequency dependent coefficient of the damping term in the differential equation.

The stress at any point in the beam is assumed to consist of two parts, one directly proportional to strain and the other dependent upon the strain rate:

$$\sigma(y) = E\left[\epsilon(y) + H\cdot\epsilon(y)\right] \tag{14}$$

where H is a time differential operator of unknown order, and $\epsilon(y)$ is the extensional strain which varies with distance y from the neutral axis of the bar.

The relation between the strain and curvature in a beam under flexure is derived by Timoshenko [Reference (13)]. For small lateral displacements of the beam, the strain-curvature relation is

$$\epsilon(y) = y\,\frac{\partial^2 u_e}{\partial x^2} \tag{15}$$

The total bending moment acting on a cross-section of the beam is related to stress as follows [Reference (13)]:

$$M_1 = \int_A \sigma(y)\, y\, dA \tag{16}$$

Combining equations 14, 15 and 16 and making the substitution that $I_z = \int_A y^2 \, dA$, we find that

$$M_1 = \int_A E\left[y + yH\right] y \frac{\partial^2 u_e}{\partial x^2} \, dA = EI_z (1+H) \frac{\partial^2 u_e}{\partial x^2}$$

The Bernoulli-Euler beam equation for forced vibration, equation 3, may now be written as follows:

$$EI_z (1+H) \frac{\partial^4 u_e}{\partial x^4} + \rho A \frac{\partial^2 u_e}{\partial t^2} = -\rho A \, D(x) \ddot{f}(t) \tag{17}$$

The preceding equation is solved by assuming that the displacement of the beam can be described as a summation of normal mode responses

$$u_e(x,t) = \sum_{n=1}^{\infty} \Phi_n(\beta_n x) \eta_n(t) \tag{18}$$

where $\Phi_n(\beta_n x)$ is the normal function derived from the differential equation for free vibration of the undamped beam, equation 6. This function can be used with the equation for a damped beam without introducing appreciable error because the mode shape of the beam is not influenced significantly by damping of small magnitude. Substituting the assumed solution, equation 18, into equation 17, and using equation 6, the differential equation becomes

$$\sum_{n=1}^{\infty} \left[EI_z \beta_n^4 (1+H) \, \Phi_n(\beta_n x) \eta_n(t) + \rho A \, \Phi_n(\beta_n x) \ddot{\eta}_n(t) \right] = -\rho A \, D(x) \ddot{f}(t)$$

Dividing through the equation by ρA and substituting the relation of equation 7:

$$\sum_{n=1}^{\infty} \left[\Phi_n(\beta_n x) \ddot{\eta}_n + \omega_n^2 (1+H) \, \Phi_n(\beta_n x) \eta_n \right] = -D(x) \ddot{f}(t) \tag{19}$$

Multiplying both sides of the equation by the integrating factor $\int_0^l \Phi_m(\beta_m x)\, dx$ and making use of the orthogonality relations we obtain

$$\ddot{\eta}_n + \omega_n^2 H \eta_n + \omega_n^2 \eta_n = \frac{\int_0^l D(x)\, \ddot{f}(t)\, \Phi_n(\beta_n x)\, dx}{\int_0^l \Phi_n^2(\beta_n x)\, dx} \tag{20}$$

The parameter H is the differential operator which introduces the dependency on strain rate. Without defining explicitly the nature of this dependency, we can determine its overall effect experimentally by writing the left side of equation 20 in the form of the differential equation of a single degree-of-freedom system with viscous damping:

$$\ddot{\eta}_n + \lambda_n \dot{\eta}_n + \omega_n^2 \eta_n = Q_n(t) \tag{21}$$

where λ_n is to be determined experimentally. The generalized force in equation 21 is

$$Q_n(t) = \frac{\ddot{f}(t) \int_0^l D(x)\, \Phi_n(\beta_n x)\, dx}{\int_0^l \Phi_n^2(\beta_n x)\, dx} \tag{22}$$

To evaluate the numerator in equation 22 it is necessary to define the rigid body displacement, D(x). Assume that the displacement at the pinned end of the beam varies sinusoidally in time; then

$$D(l) = D_o \sin \omega t \tag{23}$$

where D_o is the displacement amplitude. To produce this displacement at the pinned end a force is required, say $F(t) = F_o \sin \omega t$, where the magnitude of the force (F_o) is undefined. In addition assume the displacement of the center of mass and the rotation about the center of mass (Figure II) of the beam are given respectively by the following

expressions:

$$Y = Y_o \sin \omega t$$
$$\Theta = \Theta_o \sin \omega t \tag{24}$$

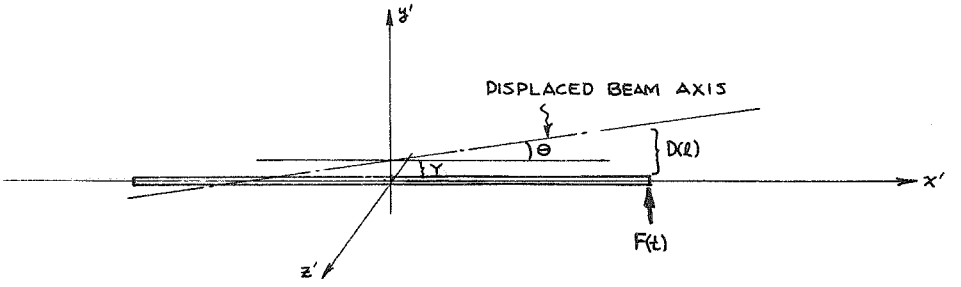

Figure II: Diagram of the free-pinned beam showing the force F(t) producing the displacement D(ℓ) at the pinned end. Shown also are the coordinate axes x', y' and z', and the independent variables Y and Θ that define respectively the translational and rotational motion about the center of mass of the beam.

The equations of translational and rotational motion are, respectively

$$F(t) = M\ddot{Y} \tag{25a}$$
$$F(t) \cdot \ell/2 = I\ddot{\Theta} \tag{25b}$$

where M is the mass of the beam and I is the mass moment of inertia of the beam about the z' axis. Under the assumption of sinusoidal excitation, the functions F(t), Y and Θ have been defined and equations 25a and 25b reduce to

$$F_o = MY_o\omega^2 \tag{26a}$$
$$F_o \cdot \frac{\ell}{2} = I\Theta_o\omega^2 \tag{26b}$$

Combining equations 26a and 26b by eliminating F_o, and making the additional substitution that $I = \frac{M\ell^2}{12}$, we obtain

$$\Theta_o = \frac{6Y_o}{\ell}$$

The displacement amplitude at any station x' is then

$$D(x') = Y_o + x'\Theta_o = Y_o + 6Y_o\frac{x'}{\ell} \tag{27}$$

To evaluate Y_o, the boundary condition is imposed that at $x' = \ell/2$, $D(x') = D_o$ as defined by equation 23. Hence from equation 27:

$$Y_o = \frac{D_o}{4}$$

Substituting this result into equation 27 and transforming to the original coordinate system ($x = x' + \ell/2$, $y = y'$, $z = z'$) with origin at the free end of the beam:

$$D(x) = \frac{D_o}{4}\left[1 + \frac{6}{\ell}\left(x - \frac{\ell}{2}\right)\right] \tag{28}$$

The generalized force $Q_n(t)$ defined by equation 22 can now be evaluated:

$$Q_n(t) = \frac{D_o\ddot{f}(t)\int_o^\ell\left[1 + \frac{6}{\ell}\left(x - \frac{\ell}{2}\right)\right]\Phi_n(\beta_n x)\,dx}{4\int_o^\ell \Phi_n^2(\beta_n x)\,dx} \tag{29}$$

For the normal function defined by equation 11 the following integral relation is obtained (see Appendix B):

$$\int_o^\ell x\,\Phi_n(\beta_n x)\,dx = \ell\int_o^\ell \Phi_n(\beta_n x)\,dx$$

Thus, the expression for the generalized force reduces to the following:

$$Q_n(t) = -\frac{D_o\ddot{f}(t)\int_o^\ell \Phi_n(\beta_n x)\,dx}{\int_o^\ell \Phi_n^2(\beta_n x)\,dx} \tag{30}$$

In equation 30 the rigid body inertia loading is represented by the term $D_o\ddot{f}(t)$ which is not space dependent. Hence, the effective inertia loading caused by the displacement $D_o \sin\omega t$ applied at the pinned end of the beam is time dependent and uniform along the beam length. The integrals in equation 30 when evaluated using equation 11

result in the following:

$$\int_0^{\ell} \Phi_n(\beta_n x)\, dx = \frac{2\zeta_n}{\beta_n} C_{1n}$$

$$\int_0^{\ell} \Phi_n^2(\beta_n x)\, dx = \ell\, C_{1n} \tag{31}$$

where

$$\zeta_n = \frac{\sin\beta_n\ell \sinh\beta_n\ell}{\sin\beta_n\ell + \sinh\beta_n\ell} \tag{32}$$

Thus, equation 30 becomes

$$Q_n(t) = \frac{2D_o\zeta_n}{\beta_n\ell\, C_{1n}} \ddot{f}(t) \tag{33}$$

The response of the free-pinned beam to the generalized force $Q_n(t)$ defined by equation 33 is to be determined. Kármán and Biot [Reference (14)] derive the integral equation for the response of a linear system to a generalized forcing function $g_n(t)$ in terms of the response of the system to a unit impulse $h_n(t)$ as follows:

$$r_n(t) = \int_0^t h_n(t-\tau)\, g_n(\tau)\, d\tau \tag{34}$$

We want the expression for $h_n(t)$ when the differential equation for the system is of second order and of the form of the left side of equation 21, i.e.

$$\ddot{r}_n(t) + \lambda_n \dot{r}_n(t) + \omega_n^2 r_n(t) = P_n(t) \tag{35}$$

First let us calculate the solution to equation 35 when the forcing function $P_n(t)$ is a unit step function having the following properties:

$$P_n(t) = 0 \qquad t < 0$$

$$P_n(t) = 1 \qquad t > 0$$

In addition, the initial conditions are

$$r_n = 0 \quad \text{at} \quad t=0$$

$$\dot{r}_n = 0 \quad \text{at} \quad t=0$$

Within the frame work of the above conditions on the force and initial motion, the solution to equation 35 is

$$r_n(t) = \frac{1}{\omega_n^2}\left[1 - e^{-\frac{\lambda_n}{2}t}\cos\sqrt{\omega_n^2-(\tfrac{\lambda_n}{2})^2}\,t - \frac{\lambda_n e^{-\frac{\lambda_n}{2}t}}{2\sqrt{\omega_n^2-(\tfrac{\lambda_n}{2})^2}}\sin\sqrt{\omega_n^2-(\tfrac{\lambda_n}{2})^2}\,t\right] \tag{36}$$

Equation 36 represents the response of a system defined by equation 34 to a unit step forcing function. The derivative of equation 36 with respect to time is the system response to a unit impulse:

$$h_n(t) = \frac{dr_n}{dt} = \frac{e^{-\frac{\lambda_n}{2}t}}{\sqrt{\omega_n^2-(\tfrac{\lambda_n}{2})^2}}\sin\sqrt{\omega_n^2-(\tfrac{\lambda_n}{2})^2}\,t \tag{37}$$

Having determined $h_n(t)$ and substituting the generalized force for the free-pinned beam $Q_n(t)$ for $q_n(t)$ in equation 34, we can write the integral solution for $\eta_n(t)$ as follows:

$$\eta_n(t) = \frac{2D_o S_n e^{-\frac{\lambda_n}{2}t}}{\beta_n \ell\, C_{in}\sqrt{\omega_n^2-(\tfrac{\lambda_n}{2})^2}}\int_0^t \ddot{f}(\tau)\, e^{\frac{\lambda_n}{2}\tau}\sin\sqrt{\omega_n^2-(\tfrac{\lambda_n}{2})^2}\,(t-\tau)\,d\tau \tag{38}$$

In accordance with the rigid body analysis, see equations 23 and 24, we take $f(\tau) = \sin\omega\tau$. Then integrating the above equation and taking the limit as $t\to\infty$, the steady state response of the beam is obtained:

$$\eta_{n_{ss}}(t) = \frac{2D_o S_n}{\beta_n \ell\, C_{in}}\frac{\omega^2}{\sqrt{(\omega^2-\omega_n^2)^2+\lambda_n^2\omega^2}}\sin(\omega t-\varphi_n) \tag{39}$$

where

$$\varphi_n = \tan^{-1}\frac{\lambda_n\omega}{(\omega_n^2-\omega^2)}$$

The steady state elastic displacement is obtained by substituting

equation 39 into equation 18. The result is

$$u_e(x,t) = \frac{2D_o}{\ell}\sum_{n=1}^{\infty} \frac{\varphi_n}{\beta_n\sqrt{\left[1-\frac{\omega_n^2}{\omega^2}\right]^2+\frac{\lambda_n^2}{\omega^2}}} \frac{\Phi_n(\beta_n x)}{C_{1n}} \sin(\omega t-\varphi_n) \tag{40}$$

The outer fiber strain at any station x along the length of the beam may be determined by substituting equation 40 into equation 15 and letting y = c. Hence,

$$\epsilon(x,c) = \frac{D_o c}{\ell}\sum_{n=1}^{\infty} \frac{2\varsigma_n\beta_n}{\sqrt{\left[1-\frac{\omega_n^2}{\omega^2}\right]^2+\frac{\lambda_n^2}{\omega^2}}} \frac{\Phi_n''(\beta_n x)}{C_{1n}} \sin(\omega t-\varphi_n) \tag{41}$$

where c is the half thickness of the beam and the term $\Phi_n''(\beta_n x)$ denotes two derivatives of $\Phi_n(\beta_n x)$ with respect to $\beta_n x$. The maximum value of the outer fiber strain at station x is obtained when $\omega t-\varphi_n = \pi/2$:

$$\epsilon_m(x,c) = \frac{D_o c}{\ell}\sum_{n=1}^{\infty} \frac{2\varsigma_n\beta_n}{\sqrt{\left[1-\frac{\omega_n^2}{\omega^2}\right]^2+\frac{\lambda_n^2}{\omega^2}}} \frac{\Phi_n''(\beta_n x)}{C_{1n}} \tag{42}$$

This equation will be used later to evaluate the λ_n for five flexural modes of vibration of a test beam in which D_o and $\epsilon_m(x,c)$ were measured at each beam resonance.

B. DERIVATION OF THE RESPONSE EQUATION FOR A FREE-PINNED BEAM EXCITED BY A RANDOM DISPLACEMENT AT THE PINNED END

1. Bandwidth of Excitation Frequencies: $0 < \omega \leq \infty$

In this section, the motion at the driven or pinned end is considered to be a stationary random process defined by a spectrum of mean squared acceleration density that is flat between the indicated limits of frequency. The probability of occurrence of instantaneous values of acceleration in the excitation and strain in the response are assumed to be normal or Gaussian [Reference (15)]. In contrast

to the previous analysis involving sinusoidal excitation, wherein both the excitation and the response are deterministic, the values of neither the excitation nor response at a given time can be predicted when the excitation is random. However, the probability of occurrence of such values can be stated, as well as their respective mean squared values. If the responding system is lightly damped, the response is in the nature of a random sine wave (narrow band random vibration) whose amplitude varies slowly with time. A multiple degree-of-freedom system responds in this manner in each normal mode, and such responses may be superimposed. Thus, the preceding analysis involving the response of the beam to sinusoidal excitation becomes applicable to random excitation if the excitation and response are properly defined.

The particular solution for the elastic displacement of the free-pinned beam was assumed to be of the form

$$u_e(x,t) = \sum_{n=1}^{\infty} \Phi_n(\beta_n x)\, \eta_n(t) \tag{18}$$

where the integral solution for $\eta_n(t)$ may be written by replacing $A_n(t)$ by $\eta_n(t)$ and $g_n(\tau)$ by $Q_n(\tau)$ in equation 34.

$$\eta_n(t) = \int_0^t h_n(t-\tau)\, Q_n(\tau)\, d\tau \tag{43}$$

First let us consider the mean squared elastic displacement of the beam. This quantity may be defined directly from equation 18 as follows:

$$\langle u_e^2(x,t) \rangle_{av} = \sum_{n=1}^{\infty} \sum_{m=1}^{\infty} \Phi_n(\beta_n x)\, \Phi_m(\beta_m x)\, \langle \eta_n(t)\, \eta_m(t) \rangle_{av} \tag{44}$$

where $\langle \eta_n(t)\, \eta_m(t) \rangle_{av}$ is undefined, but from equation 43 we can write

$$\langle \eta_n(t)\, \eta_m(t) \rangle_{av} = \int_0^t \int_0^t \langle Q_n(\tau)\, Q_m(\tau') \rangle_{av} h_n(t-\tau)\, h_m(t-\tau')\, d\tau\, d\tau' \qquad (45)$$

Finally, it is necessary to define the mean squared expression for the generalized forcing function $\langle Q_n(\tau)\, Q_m(\tau') \rangle_{av}$. The generalized forcing function for the free-pinned beam was derived in the previous section:

$$Q_n(t) = \frac{2 D_o \delta_n}{\beta_n \ell\, C_m} \ddot{f}(t) \qquad (33)$$

Replacing the variable t by τ as required in equation 45, the mean square of $Q_n(\tau)$ (equation 33) is

$$\langle Q_n(\tau)\, Q_m(\tau') \rangle_{av} = \frac{\delta_n \delta_m}{\beta_n \beta_m \ell^2 C_m C_{1m}} 4 D_o^2 \langle \ddot{f}(\tau)\, \ddot{f}(\tau') \rangle_{av} \qquad (46)$$

Assume that the beam is subjected to a stationary random Gaussian excitation having a constant mean squared acceleration spectral density over the frequency range from 0 to ∞. In addition, assume the only correlation in time occurs when $\tau = \tau'$; then we can write

$$4 D_o^2 \langle \ddot{f}(\tau)\, \ddot{f}(\tau') \rangle_{av} = \frac{G}{2} \delta(\tau - \tau') \qquad (47)$$

where G is a constant that represents the value of the mean squared acceleration spectral density of the forcing function, and $\delta(\tau - \tau')$ is the Dirac Delta function which has the properties

$$\delta(\tau - \tau') = 0 \qquad \tau \neq \tau'$$

$$\delta(\tau - \tau') = 1 \qquad \tau = \tau'$$

Substituting equation 47 into equation 46:

$$\langle Q_n(\tau)\, Q_m(\tau') \rangle_{av} = \frac{\delta_n \delta_m G}{2 \beta_n \beta_m \ell^2 C_m C_{1m}} \delta(\tau - \tau') \qquad (48)$$

Equation 48 can now be substituted into equation 45:

$$\langle \eta_n(t)\,\eta_m(t)\rangle_{av} = \frac{G}{2l^2}\int_0^t\int_0^t \frac{S_n S_m}{\beta_n\beta_m C_n C_m}\,\delta(\tau-\tau')\,h_n(t-\tau)\,h_m(t-\tau')\,d\tau\,d\tau' \qquad (49)$$

The impulse response functions $h_n(t-\tau)$ and $h_m(t-\tau')$ in equation 49 may be defined using equation 37. Therefore, one integration of equation 49 results in the following:

$$\langle \eta_n(t)\,\eta_m(t)\rangle_{av} = \frac{G S_n S_m}{2\beta_n\beta_m l^2 C_n C_m}\int_0^t \frac{e^{-\frac{\lambda_n}{2}(t-\tau)}}{\sqrt{\omega_n^2-(\frac{\lambda_n}{2})^2}}\;\frac{e^{-\frac{\lambda_m}{2}(t-\tau)}}{\sqrt{\omega_m^2-(\frac{\lambda_m}{2})^2}}$$

$$\cdot \sin\sqrt{\omega_n^2-(\tfrac{\lambda_n}{2})^2}\,(t-\tau)\;\sin\sqrt{\omega_m^2-(\tfrac{\lambda_m}{2})^2}\,(t-\tau)$$

Upon further reduction of this equation using trigonometric identities it is found that the integration can be separated into several parts, each part being of the form

$$\int_0^t e^{a\tau}\sin b\tau\,d\tau \qquad \text{or} \qquad \int_0^t e^{a\tau}\cos b\tau\,d\tau$$

These integrals are listed in standard integral tables [Reference (16)]. Performing the integration, we find for the total response the following:

$$\langle \eta_n(t)\eta_m(t)\rangle_{av} = \frac{S_n S_m G}{2\beta_n\beta_m l^2 C_n C_m}\left[\frac{e^{-at}}{b_n b_m}\left\{\sin\left[(b_n+b_m)t-\theta_1\right]-\sin\left[(b_n-b_m)t-\theta_2\right]\right\}\right.$$

$$\left.+\frac{2(\lambda_n+\lambda_m)}{(\omega_n^2-\omega_m^2)^2+\lambda_n^2\omega_m^2+\lambda_m^2\omega_n^2+\lambda_n\lambda_m(\omega_n^2+\omega_m^2)}\right] \qquad (50)$$

The undefined terms in equation 50 are

$$a = \tfrac{1}{2}(\lambda_n+\lambda_m) \qquad (51)$$

$$b_m = \sqrt{\omega_m^2-(\tfrac{\lambda_m}{2})^2} \qquad (52a)$$

$$b_n = \sqrt{\omega_n^2-(\tfrac{\lambda_n}{2})^2} \qquad (52b)$$

$$\Theta_1 = \sin^{-1}\frac{a}{\left[(b_n+b_m)^2+a^2\right]^{1/2}} \tag{53}$$

$$\Theta_2 = \sin^{-1}\frac{a}{\left[(b_n-b_m)^2+a^2\right]^{1/2}} \tag{54}$$

The mean squared steady-state response is obtained when $t \to \infty$. Hence,

$$\lim_{t\to\infty} \langle \eta_n(t)\, \eta_m(t) \rangle_{av} \equiv \langle \eta_n(t)\, \eta_m(t) \rangle_{av_{ss}} =$$

$$\frac{\mathcal{F}_n \mathcal{F}_m G}{2\beta_n\beta_m \ell^2 C_{1n} C_{1m}} \left[\frac{\lambda_n+\lambda_m}{(\omega_n^2-\omega_m^2)^2+(\lambda_n+\lambda_m)(\lambda_n\omega_m^2+\lambda_m\omega_n^2)} \right] \tag{55}$$

The steady-state mean squared displacement is obtained by substituting equation 55 into equation 44. The result is

$$\langle u_e^2(x,t) \rangle_{av} = \frac{G}{2\ell^2} \sum_{n=1}^{\infty}\sum_{m=1}^{\infty} \frac{\mathcal{F}_n\mathcal{F}_m}{\beta_n\beta_m} \left[\frac{\lambda_n+\lambda_m}{(\omega_n^2-\omega_m^2)^2+(\lambda_n+\lambda_m)(\lambda_n\omega_m^2+\lambda_m\omega_n^2)} \right] \frac{\Phi_n(\beta_n x)}{C_{1n}} \frac{\Phi_m(\beta_m x)}{C_{1m}} \tag{56}$$

If the natural frequencies of the beam are separated sufficiently there is negligible cross-coupling and equation 56 reduces to the following:

$$\langle u_e^2(x,t) \rangle_{av} = \frac{G}{2\ell^2} \sum_{n=1}^{\infty} \frac{\mathcal{F}_n^2}{\omega_n^2 \lambda_n \beta_n^2} \frac{\Phi_n^2(\beta_n x)}{C_{1n}^2} \tag{57}$$

Finally, the mean squared outer fiber strain at any station x along the beam can be calculated using equation 15 and letting y = c. Substituting equation 18 into equation 15, the strain is

$$\epsilon(x,c) = c \sum_{n=1}^{\infty} \beta_n^2\, \Phi_n''(\beta_n x)\, \eta_n(t)$$

where the term $\Phi_n''(\beta_n x)$ denotes two derivatives of $\Phi_n(\beta_n x)$ with respect to its argument. Therefore, the mean squared outer fiber strain is:

$$\overline{\epsilon^2(x,c)} = c^2 \sum_{n=1}^{\infty}\sum_{m=1}^{\infty} \beta_n^2\beta_m^2\, \Phi_n''(\beta_n x)\, \Phi_m''(\beta_m x) \langle \eta_n(t)\, \eta_m(t) \rangle_{av}$$

or, using equation 50, its steady-state value is:

$$\overline{\epsilon^2(x,c)} = \frac{c^2G}{2\ell^2}\sum_{n=1}^{\infty}\sum_{m=1}^{\infty} \frac{\beta_n\beta_m \zeta_n\zeta_m (\lambda_n+\lambda_m)}{(\omega_n^2-\omega_m^2)^2+(\lambda_n+\lambda_m)(\lambda_n\omega_m^2+\lambda_m\omega_n^2)} \frac{\Phi_n''(\beta_n x)}{C_{1n}} \frac{\Phi_m''(\beta_m x)}{C_{1m}} \qquad (58)$$

If there is negligible coupling between modes, equation 58 reduces to the following:

$$\overline{\epsilon^2(x,c)} = \frac{c^2G}{2\ell^2}\sum_{n=1}^{\infty} \frac{\beta_n^2\zeta_n^2}{\omega_n^2\lambda_n} \frac{\left[\Phi_n''(\beta_n x)\right]^2}{C_{1n}^2} \qquad (59)$$

To test whether this series is convergent, we can make the following substitution

$$\omega_n^2 = \beta_n^4 \frac{EI_z}{\rho A} \qquad (7)$$

In addition $\zeta_n \simeq \frac{\sqrt{2}}{2}$ (see Table I on page 38). From beam tables [Reference (17)] we know that for a free-pinned beam the values of $\frac{[\Phi_n''(\beta_n x)]^2}{C_{1n}^2}$ vary from 0 to 4 and hence may be assumed of order unity. Further,

$$\beta_n\ell \simeq \frac{\pi}{4}(4n+1) \qquad (n>5)$$

where n is the mode number. The damping coefficient λ_n is generally proportional to some function of the frequency:

$$\lambda_n \sim \omega_n^{\alpha} \qquad (\alpha > 0)$$

Making these substitutions into equation 59 and neglecting the constant parameters, we find that the mean squared strain is proportional to the following series:

$$\overline{\epsilon^2} \sim \sum_{n}^{\infty} \frac{1}{n^{2(1+\alpha)}} \qquad \text{(for n large)}$$

This series converges absolutely.

2. Bandwidth of Excitation Frequencies: $0 < \omega < \omega_c$

In the previous analysis we considered a flat mean squared

acceleration spectrum; i.e., the acceleration spectral density was constant over the frequency range $0 < \omega < \omega_c$. Consider now a flat acceleration spectrum that is clipped at frequency ω_c (see Figure III).

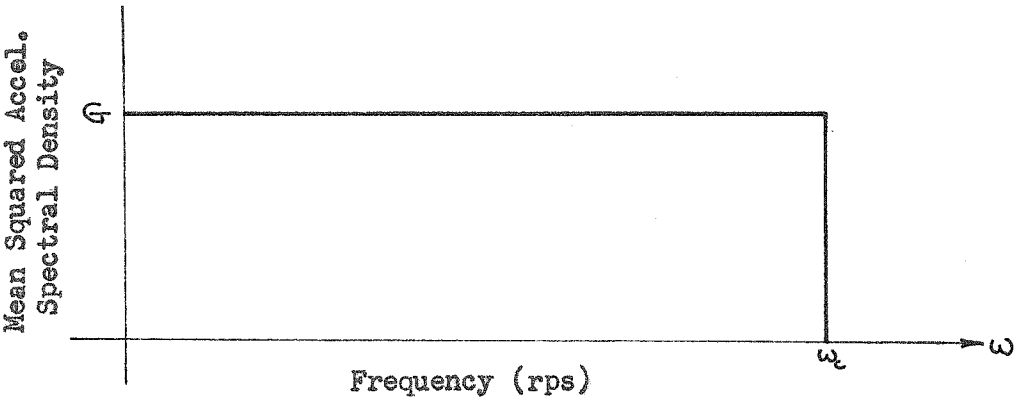

Figure III: Example of a clipped spectrum of mean squared acceleration.

One reason for considering this type of spectrum is that a clipped spectrum is a more accurate representation of the type generated by electromechanical shake table systems. Generally, the cutoff frequency of the spectrum is placed below the lowest axial resonant frequency of the shake table armature. A method derived by Thomson and Barton [Reference (6)] will be used to obtain the steady-state mean squared elastic displacement of the free-pinned beam. In reference (6) the authors express the mean squared displacement in terms of the impedance function $Z(\omega)$ for a beam and the mean squared acceleration spectral density $\Phi(\omega)$ of the excitation as follows:

$$\overline{u^2} = \int \frac{\Phi(\omega)\, d\omega}{|Z(\omega)|^2} \tag{60}$$

where $\Phi(\omega)$ and $Z(\omega)$ are related to the correlation function

(equation 47) and unit impulse response (equation 37) as follows [Reference (15)]:

$$\Phi(\omega) = \frac{2}{\pi}\int_0^\infty \frac{G}{2}\,\delta(\tau)\cos\omega\tau\,d\tau = \frac{G}{2\pi} \tag{61}$$

and

$$\frac{1}{Z(\omega)} = \sum_{n=1}^{\infty} \frac{S_n \Phi_n(\beta_n x)}{\beta_n l\, C_{in}} \int_0^t h_n(\tau)\, e^{-i\omega\tau}\, d\tau \tag{62}$$

But from equation 37 we know that

$$h_n(\tau) = \frac{e^{-a_n\tau}}{b_n}\sin b_n\tau$$

where

$$a_n = \frac{\lambda_n}{2} \quad , \qquad b_n = \sqrt{\omega_n^2 - \left(\frac{\lambda_n}{2}\right)^2}$$

Therefore, integration of equation 62 results in

$$\frac{1}{Z(\omega)} = \sum_{n=1}^{\infty} \frac{S_n \Phi_n(\beta_n x)}{\beta_n l\, C_{in}} \frac{1}{\left[\omega_n^2 - \omega^2 + i\omega\lambda_n\right]} \tag{63}$$

The square of the absolute value of equation 63 is then

$$\frac{1}{|Z(\omega)|^2} = \sum_{n=1}^{\infty}\sum_{m=1}^{\infty} \frac{S_n S_m}{\beta_n \beta_m l^2} \frac{\Phi_n(\beta_n x)}{C_{in}} \frac{\Phi_m(\beta_m x)}{C_{im}} \frac{1}{\left[(\omega_n^2-\omega^2)^2 + \lambda_n^2\omega^2\right]^{1/2}\left[(\omega_m^2-\omega^2)^2 + \lambda_m^2\omega^2\right]^{1/2}} \tag{64}$$

Thomson and Barton (6) derive equation 64 directly from the equation of motion for a beam. Substituting equations 61 and 64 into equation 60, we obtain

$$\overline{u_e^2} = \frac{G}{2\pi}\sum_{n=1}^{N}\sum_{m=1}^{M} \frac{S_n S_m \Phi_n(\beta_n x)\Phi_m(\beta_m x)}{\beta_n \beta_m l^2 C_{in} C_{im}} \int_0^{\omega_c} \frac{d\omega}{\left[(\omega_n^2-\omega^2)^2 + \lambda_n^2\omega^2\right]^{1/2}\left[(\omega_m^2-\omega^2)^2 + \lambda_m^2\omega^2\right]^{1/2}} \tag{65}$$

where the limits of the integration are from zero to ω_c since the mean squared acceleration spectral density (G) is zero for $\omega > \omega_c$. The summation is also modified since only those modes of the beam with

natural frequencies below ω_c will be excited. This condition can be expressed as follows:

$$\omega_M < \omega_c$$

$$\omega_N < \omega_c$$

Assume further that cross coupling between modes is negligible; then equation 65 reduces to

$$\overline{u_e^2} = \frac{G}{2\pi} \sum_{n=1}^{N} \frac{S_n^2 \, \Phi_n^2(\beta_n x)}{\beta_n^2 \ell^2 C_{1n}^2} \int_0^{\omega_c} \frac{d\omega}{\left[(\omega_n^2 - \omega^2)^2 + \lambda_n^2 \omega^2\right]}$$

The integral in this equation is listed in tables [Reference (16)]. The result of integration is

$$\overline{u_e^2} = \frac{G}{2\pi \ell^2} \sum_{n=1}^{N} \frac{S_n^2}{\omega_n^2 \lambda_n \beta_n^2} \frac{\Phi_n^2(\beta_n x)}{C_{1n}^2} \left[\frac{\lambda_n}{\sqrt{4\omega_n^2 - \lambda_n^2}} \ln \frac{\omega_c^2 + \omega_n^2 + \omega_c \sqrt{4\omega_n^2 - \lambda_n^2}}{\omega_c^2 + \omega_n^2 - \omega_c \sqrt{4\omega_n^2 - \lambda_n^2}} \right.$$

$$\left. + \tan^{-1} \frac{2\omega_c - \sqrt{4\omega_n^2 - \lambda_n^2}}{\lambda_n} + \tan^{-1} \frac{2\omega_c + \sqrt{4\omega_n^2 - \lambda_n^2}}{\lambda_n} \right] \qquad (66)$$

In the limit as $\omega_c \to \infty$, equation 64 should reduce to equation 57. Hence, letting $\omega_c \to \infty$ we find that

$$\lim_{\omega_c \to \infty} \left[\ln \frac{1 + \frac{\omega_n^2}{\omega_c^2} + \frac{\sqrt{4\omega_n^2 - \lambda_n^2}}{\omega_c}}{1 + \frac{\omega_n^2}{\omega_c^2} - \frac{\sqrt{4\omega_n^2 - \lambda_n^2}}{\omega_c}} \right] = \ln 1 = 0$$

$$\lim_{\omega_c \to \infty} \left[\tan^{-1} \frac{2\omega_c - \sqrt{4\omega_n^2 - \lambda_n^2}}{\lambda_n} \right] = \tan^{-1} \infty = \frac{\pi}{2}$$

$$\lim_{\omega_c \to \infty} \left[\tan^{-1} \frac{2\omega_c + \sqrt{4\omega_n^2 - \lambda_n^2}}{\lambda_n} \right] = \tan^{-1} \infty = \frac{\pi}{2}$$

Therefore

$$\overline{u_c^2} = \frac{G}{2\pi\ell^2}\sum_{n=1}^{\infty} \frac{S_n^2\,\Phi_n^2(\beta_n x)}{\omega_n^2\,\lambda_n\,\beta_n^2\,C_{1n}^2}\,[\pi] = \frac{G}{2\ell^2}\sum_{n=1}^{\infty} \frac{S_n^2\,\Phi_n^2(\beta_n x)}{\omega_n^2\,\lambda_n\,\beta_n^2\,C_{1n}^2} \tag{67}$$

Equation 67 is identical to the previously derived result, equation 57. Hence, in equation 66 the term in square brackets multiplied by $1/\pi$ represents the correction factor due to clipping of the acceleration spectrum. Denoting this term by R_{cn}:

$$R_{cn} = \frac{1}{\pi}\left[\frac{\sqrt{\gamma}}{\sqrt{1-\gamma}}\,\ln\frac{1+\xi^2+2\xi\sqrt{1-\gamma}}{1+\xi^2-2\xi\sqrt{1-\gamma}}\right.$$

$$\left. + \tan^{-1}\frac{1-\xi\sqrt{1-\gamma}}{\sqrt{\gamma}} + \tan^{-1}\frac{1+\xi\sqrt{1-\gamma}}{\sqrt{\gamma}}\right] \tag{68}$$

where

$$\gamma = \frac{\lambda_n^2}{4\omega_n^2} \tag{69}$$

$$\xi = \frac{\omega_n}{\omega_c} \tag{70}$$

In the following discussion we will refer to R_{cn} as the "Clipping Correction Factor."

The result obtained in the derivation of equation 67 was that as $\omega_c \to \infty$, $R_{cn} \to 1$. Additional values of R_{cn} were calculated from equation 66 for various values of the frequency ratio ω_c/ω_n and the damping parameter γ, and the results are plotted in Figure IV. In the calculation of the curves in Figure IV an approximation was made to determine reasonable numerical values for γ. Assuming viscous type damping, $\lambda_n = 2\,C_c\,\omega_n$ and

$$\gamma = \frac{\lambda_n^2}{4\omega_n^2} = (C_c)^2 \tag{71}$$

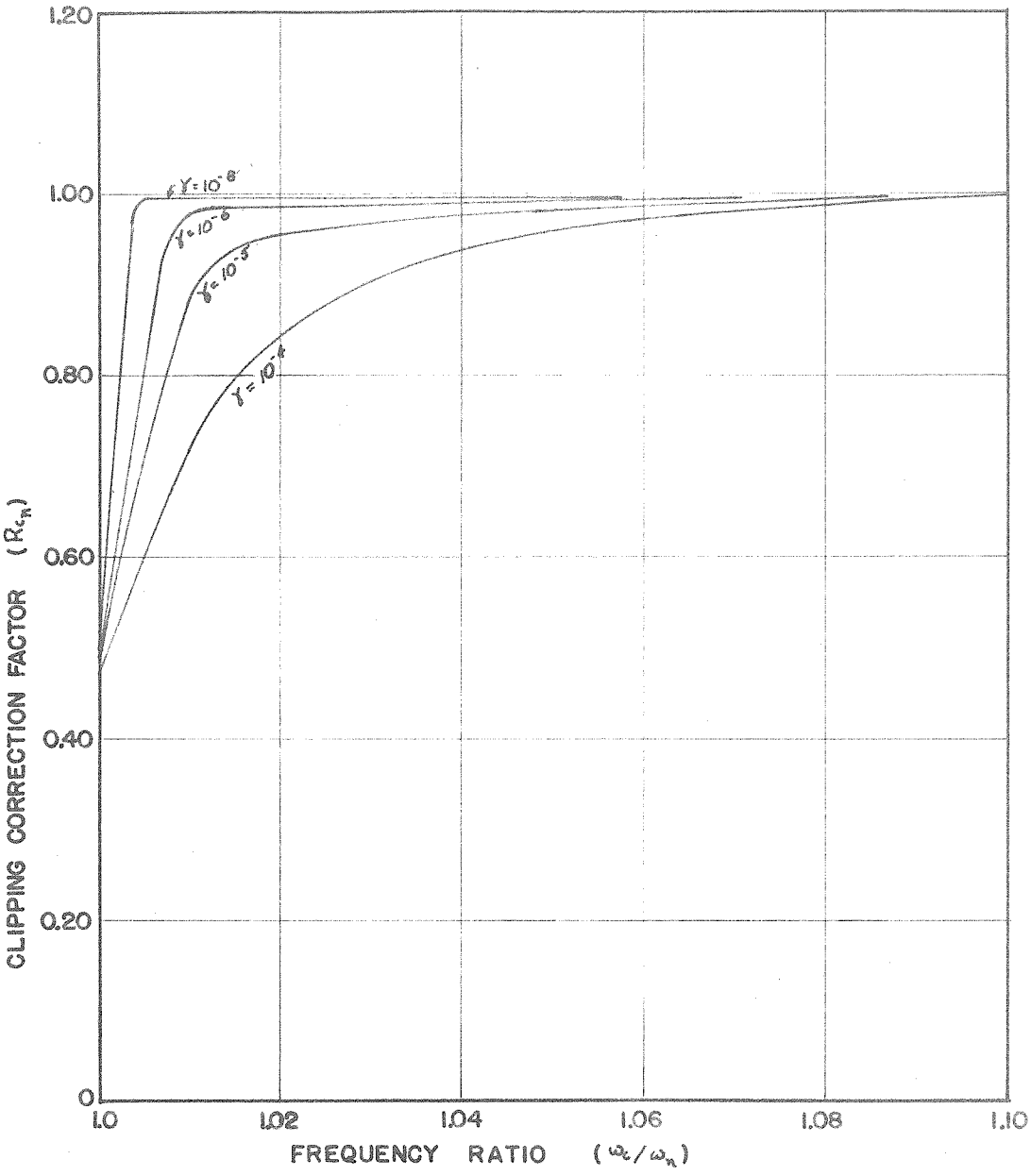

Figure IV: Plot of the clipping correction factor (R_{c_n}) versus the frequency ratio (ω_c/ω_n). The clipping correction factor is defined as the ratio of the value of the n^{th} modal contribution in the mean squared displacement response for the clipped flat spectrum to the n^{th} modal contribution in the mean squared displacement response for the flat spectrum with bandwidth $0 < \omega < \infty$. The damping parameter γ is equivalent to the square of the fraction of critical damping c/c_c (equation 71).

For a lightly damped beam, equivalent values of c/c_c may vary from 10^{-4} to 10^{-2}; based upon equation 71, the variation in γ would be from 10^{-8} to 10^{-4} respectively. The curves in Figure IV span this range of values for γ.

For a multiple degree-of-freedom system excited by a random vibration, the major contribution to the mean squared response of the system is from the area under the response curve near each resonance. The shape of the response curve of a lightly damped system in the vicinity of a resonant frequency is defined as being highly peaked (narrow bandwidth) and approximately symmetric about the resonant frequency. Hence, if the clipping cutoff frequency is placed at a resonant frequency of a system, then approximately one half of the area of the resonant curve is included in the mean squared response from that mode, which accounts for $R_{cn} = 1/2$ when $\omega_c = \omega_n$ (see Figure IV). In addition, since the resonant curves are highly peaked, only a small increase in ω_c above ω_n is sufficient to include the major portion of the area under the resonant curve. This is the reason for the rapid rise in R_{cn} with increase in the frequency ratio ω_c/ω_n in Figure IV.

Substituting R_{cn} in place of $1/\pi$ times the term in brackets in equation 66, and expanding the equation we obtain:

$$\overline{u_e^2} = R_{c_1}\overline{u_{e_1}^2} + R_{c_2}\overline{u_{e_2}^2} + R_{c_3}\overline{u_{e_3}^2} + \cdots R_{cn}\overline{u_{e_n}^2} + \cdots \qquad (72)$$

where $\overline{u_{e_1}^2}$, $\overline{u_{e_2}^2}$ etc. are the modal contributions to the mean squared displacement ($\overline{u_e^2}$) when the spectrum is flat over the frequency range

$0 < \omega < \infty$. Assume now that the cutoff frequency is placed at the resonant frequency of the second mode. Then the mean squared displacement from equation 72 is

$$\overline{u_e^2} = R_{c_1} \overline{u_{e_1}^2} + R_{c_2} \overline{u_{e_2}^2}$$

where $\overline{u_{e_n}^2} = 0$ for $n > 2$ since G is zero for $\omega_c > \omega_2$. The cutoff frequency is equal to the resonant frequency of the second mode; therefore, $R_{c_2} \simeq 1/2$ (Figure IV). However, the cutoff frequency is well above the first resonant frequency so $R_{c_1} \simeq 1.0$. Therefore, the mean squared response is

$$\overline{u_e^2} = \overline{u_{e_1}^2} + \tfrac{1}{2} \overline{u_{e_2}^2}$$

If the cutoff frequency is placed between the second and third modes so that $\omega_c > \omega_1$, and $\omega_c > \omega_2$, then the mean squared response is

$$\overline{u_e^2} = \overline{u_{e_1}^2} + \overline{u_{e_2}^2}$$

Therefore, we conclude that if the cutoff frequency of a clipped spectrum is different from the natural frequencies of the beam (by say $\omega_c/\omega_n \geq 1.1$), then all values of the R_{c_n} are equal to one. The total mean squared displacement response is then merely a summation of the modal responses, calculated using the response equation derived when the input spectrum is flat over the bandwidth $0 < \omega < \infty$, in which only those modes whose natural frequencies are below the cutoff frequency (ω_c) are included in the summation.

For a particular beam configuration all of the terms in equation 59 can be evaluated by specifying the boundary conditions except G and λ_n. The value of the mean squared acceleration spectral density (G) can be determined from a spectral analysis of the forcing

function. The value of the damping coefficients (λ_n) for each mode must be determined experimentally using equation 40 or 42. In the following section a description and the results of a test to evaluate the damping coefficients are presented.

III. EXPERIMENTAL DETERMINATION OF DAMPING

A. APPARATUS

The damping in the beam was determined by noting the magnitude of steady-state vibration of the beam at several of its natural frequencies. The variable frequency excitation was imposed at one end of the beam. The constraints on the beam, in commonly used terms are described as "free-pinned"; i.e., one end of the beam is free or unconstrained whereas the other end is constrained by a hinge or pinned joint. The beam was arranged with its length extending horizontally and its pinned end supported by the vibration testing machine used to impose the vibrating motion. Near the free end, the beam was supported by a wire positioned so that it would not participate appreciably in vibration of the beam in the modes being studied. A diagram of the test beam and its supports is shown in Figure V.

The beam was made from cold rolled steel (AISI 1018) $\frac{1}{4}$ in. x $2\frac{1}{4}$ in. in cross-section and 36 in. long. The vibration testing machine was an MB Type C-10 capable of a vector force output of 1200 lbs. varying sinusoidally from 5 to 2000 cps. The "pinned" joint was actually a flexure plate having a necked-down central portion (see Figure V) to minimize bending stiffness and approximate the frictionless hinge assumed in the analysis. The flexure was silver soldered to both the beam and the armature of the vibration testing machine to minimize damping resulting from relative motion at a joint.

With the beam extending horizontally, the pinned end was driven horizontally in the direction normal to the longitudinal axis of the beam.

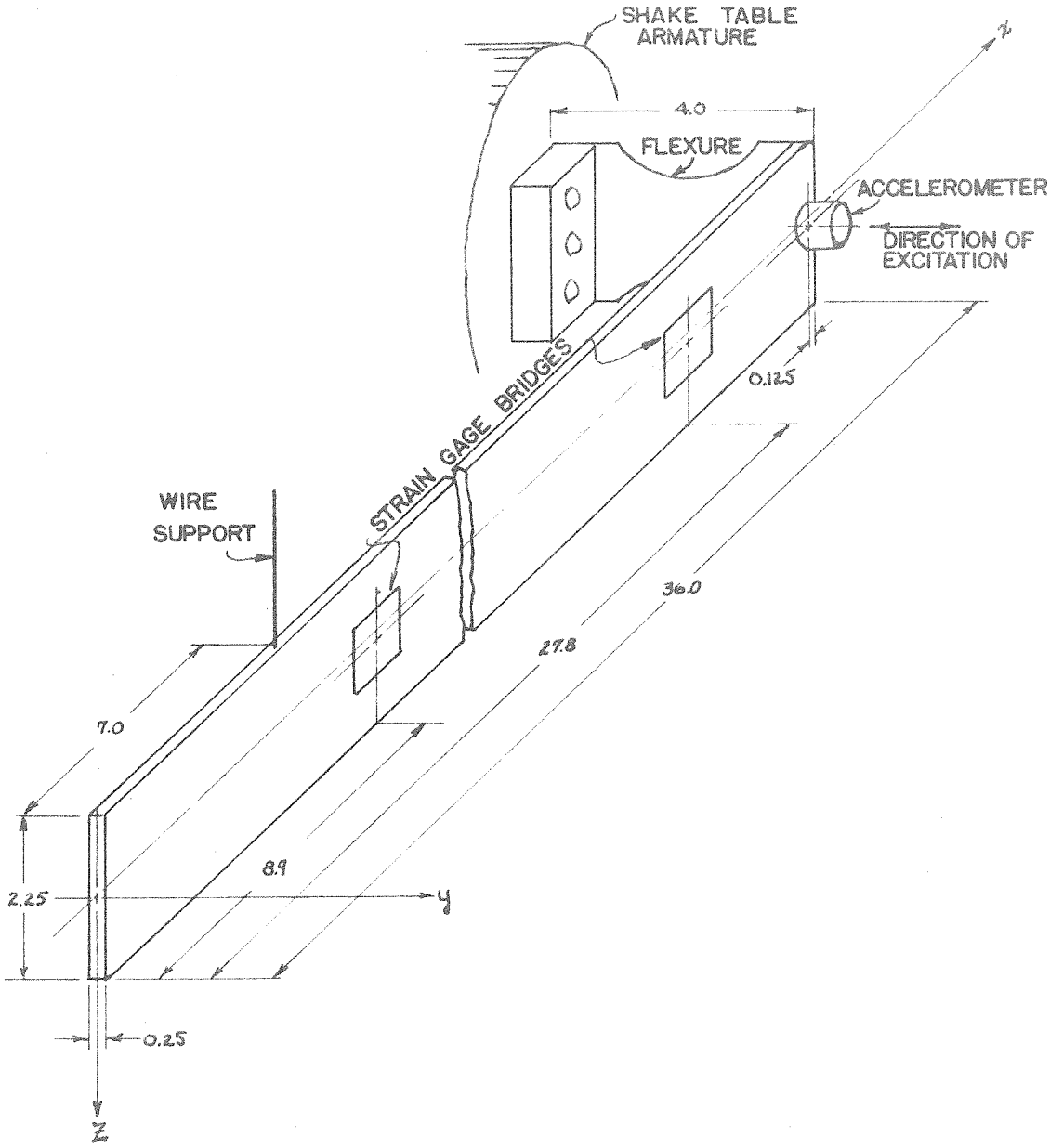

Figure V: Diagram of the test bar and its supports. The locations of the strain gage bridges and the accelerometer are indicated. All dimensions are in inches, however, the drawing is not to scale.

The frequency of the sinusoidally varying driving force was varied between 20 and 500 cps, encompassing the five lowest natural frequencies in bending modes. The cross-section of the beam was designed so that the lowest natural frequency in a bending mode in the vertical plane was greater than 500 cps, thereby minimizing the possibility of coupling between vibrations in the horizontal and vertical planes.

The motion imposed at the pinned end of the beam was measured by a piezoelectric accelerometer (model 2215, Endevco Corporation, Pasadena, California) mounted 1/8 in. from the pinned end in the center of the beam width (see Figure V). The response of the beam was measured by strain gages (SR-4, Type C-6-121) cemented to the beam. The foil type strain gages were arranged in a Wheatstone bridge (Figure VI) with adjacent gages mounted on opposite sides of the beam. This arrangement of gages resulted in measurement of four times the bending strain resulting from flexure in the horizontal plane and cancellation of any extensional or compressional strain in the beam. The strain gage positions, $x/\ell = 0.2476$ and $x/\ell = 0.772$, where ℓ is the beam length and x is the distance from the free end, were selected to maximize the participation of each strain gage bridge in all five lowest modes of vibration of the beam. The strain gage leads were made from very fine insulated copper wire, glued locally to the beam and looped loosely to a terminal box to minimize their effect on motion of the beam.

Calibration of the strain gages was achieved by shunting a calibrating resistor across one of the strain gages, as described in detail in Appendix A. The accelerometer was calibrated in a separate

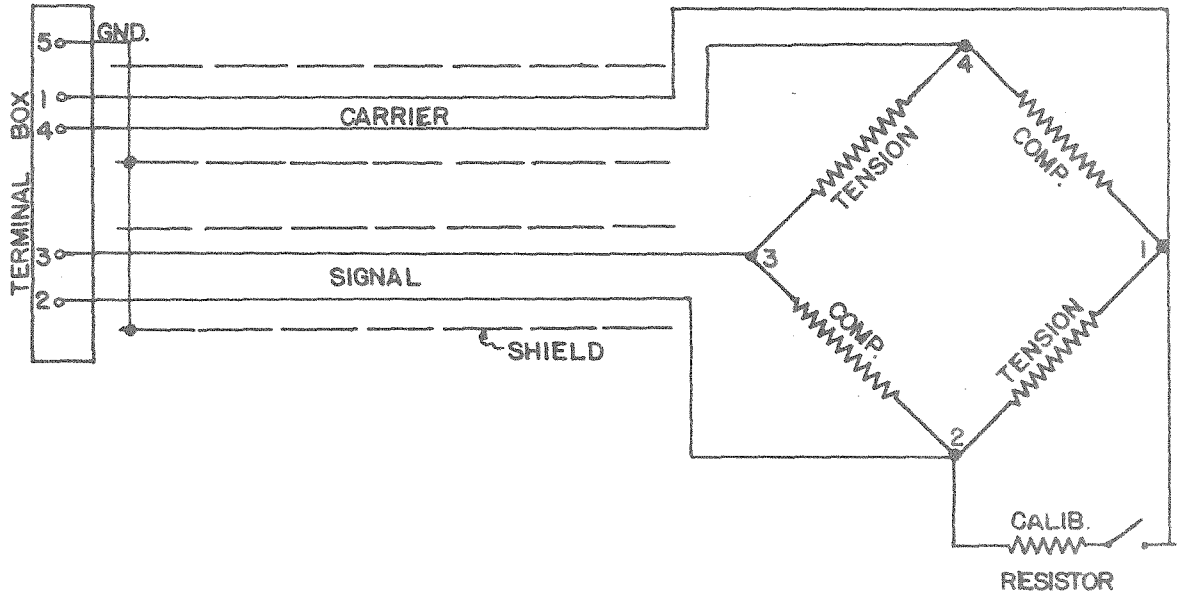

GAGE TYPE : C-6-121 (FOIL)
GAGE FACTOR: 2.01 ±.5
RESISTANCE: 120 ±.2 OHMS
LOT NUMBER: A3-E-22

CALIBRATION RESISTORS:

22,000 ± 1/20 %
44,000 ± 1/20 %
96,232 ± 1/20 %

FIGURE VI: STRAIN GAGE BRIDGE CIRCUIT

test so that the relation between the self-generated voltage output of the accelerometer and the input acceleration was known. The signals from the accelerometer and the two strain gage bridges were recorded as a function of time on a galvanometer type, multi-channel recording oscillograph (Model 590, Midwestern Recorder, Midwestern Instruments, Tulsa, Oklahoma). Figure VII shows a schematic diagram of important parts of the experimental equipment.

B. TESTING PROCEDURE

In all experiments the acceleration at the driven end of the beam and the strain at the two strain gage locations were measured simultaneously. In determining resonant curves for the beam it was the initial intention to set the excitation at a particular frequency and to measure the acceleration amplitude at the exciter and the resulting strain amplitudes at the beam for various levels of excitation. Then the frequency would be changed and the experiment repeated. Finally, a cross plotting of the assemblage of curves obtained from this experimental procedure would result in evaluation of resonant curves for constant strain output and variable displacement input. This would result in evaluation of the damping variation with variation in strain. This test procedure produced adequate data at frequencies differing somewhat from the beam natural frequencies; however, in the vicinities of the resonances, it was found impossible to maintain sufficiently close control of the shake table system to eliminate frequency drift. Because of this instability problem, the procedure in determining the resonant curves for the beam was modified. The strain output of the

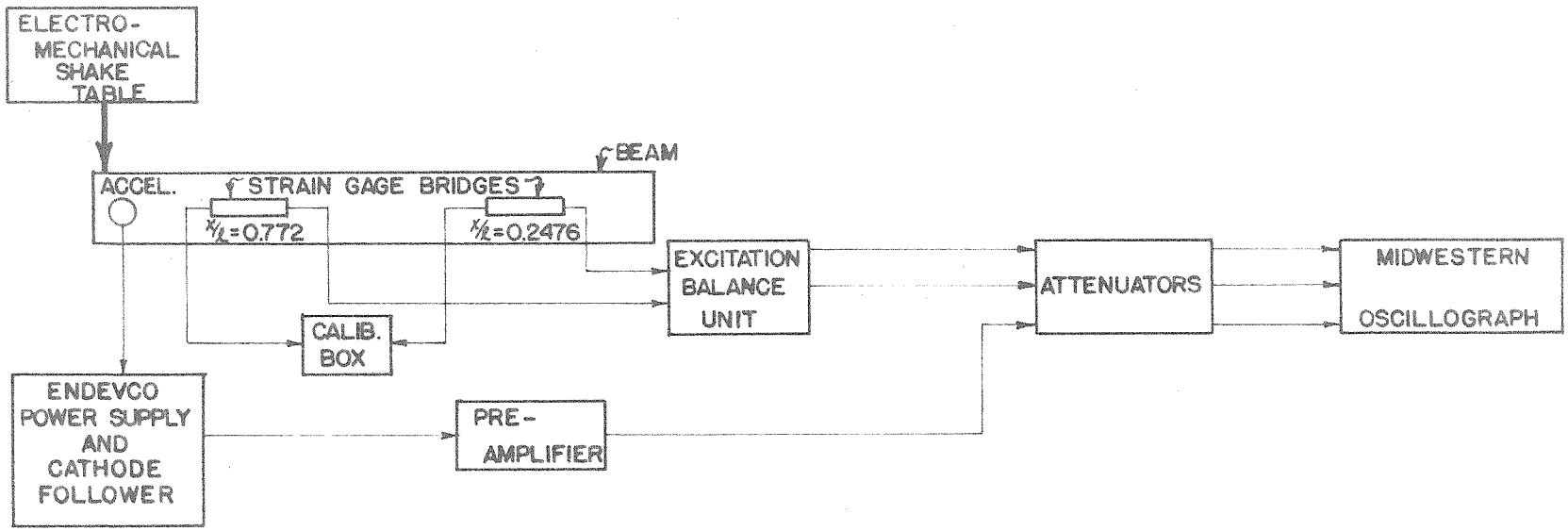

MONITORING AND CALIBRATION EQUIPMENT

BALLANTINE TRUE RMS METER	HEWLETT PACKARD OSCILLATOR	TEKTRONICS OSCILLOSCOPE

FIGURE VII: SCHEMATIC DIAGRAM OF THE EQUIPMENT SETUP FOR THE SINUSOIDAL VIBRATION TESTS

beam could be monitored by observing the swing of the galvanometer trace on the oscillograph. So for various resonant and near resonant frequencies the excitation amplitude was varied until the strain amplitude was at its pre-selected value and a recording was made. Using this procedure, response curves for the three lowest bending modes were obtained in which the strain was constant; however, the shape of the response curve in the region of resonance could not be attained satisfactorily.

To evaluate the damping at each resonance of the beam, only the amplitudes of the excitation and strain output were needed at the exact natural frequency of each mode. To overcome the difficulty of controlling the frequency, a modified procedure was adopted in which the frequency was varied slowly and continuously throughout the frequency range of interest. The shake table system that was used was equipped with a feedback servomechanism that maintained the excitation at a pre-set level while the frequency was varied continuously at a pre-set sweep rate. The sweep rate was logarithmic, i.e., at 10 cps the sweep rate was 3 cps per minute, while at 100 cps the sweep rate was 30 cps per minute etc. Thus, because of the low rate of change of frequency, the maximum response of the beam was approximately equal to that resulting from steady-state vibration at resonance. By simultaneously recording acceleration and strain, it was possible from the oscillograms to relate the strain amplitude in the beam to the acceleration amplitude at the driven end during vibration at the respective normal mode resonances. The acceleration amplitude was divided by the

square of the angular frequency, and expressed in terms of the displacement amplitude. The results for the several tests are set forth in Table III on page 43.

C. EVALUATION OF EXPERIMENTAL DATA

The objective of the experimental work was to evaluate the coefficient λ_n of the $\dot{\eta}_n$ term in equation 21. In the vicinity of each normal mode frequency ω_n, the beam responds as a damped single degree-of-freedom system. Such response is described by equation 42, giving strain amplitude as a function of the beam parameters and the excitation. Equation 42 is evaluated as follows:

$$\epsilon_m(x,c) = \frac{D_o c}{l^2} \sum_{n=1}^{\infty} \frac{2\zeta_n \beta_n l}{\sqrt{\left[1-\frac{\omega_n^2}{\omega^2}\right]^2 + \frac{\lambda_n^2}{\omega^2}}} \frac{\Phi_n''(\beta_n x)}{C_{1n}} = D_o \sum_{n=1}^{\infty} \frac{\Psi_n(\beta_n x)}{\sqrt{\left[1-\frac{\omega_n^2}{\omega^2}\right]^2 + \frac{\lambda_n^2}{\omega^2}}} \qquad (42a)$$

where: c = half thickness of beam (= 0.125 in.)

l = length of beam (= 36 in.)

β_n = beam parameter (in.$^{-1}$)(equation 7)

D_o = amplitude of displacement input (in.)

ζ_n = beam parameter depending upon beam constraints (equation 31)

λ_n = beam damping coefficient (sec.$^{-1}$)(equation 21)

ω = excitation frequency (sec.$^{-1}$)

ω_n = normal mode frequency of n^{th} mode (sec.$^{-1}$)

Φ_n = normal function (equation 11)

Ψ_n = beam parameter $\left(= \frac{2 c \beta_n l \zeta_n}{l^2} \frac{\Phi_n''(\beta_n x)}{C_{1n}} \right)$

In equation 42a several of the beam parameters must be evaluated. The values of $\beta_n l$ must satisfy the frequency equation given by equation 13; they are designated the eigenvalues for the free-pinned beam. The eigenvalues may readily be calculated by plotting

the functions $\tan \beta_n \ell$ and $\tanh \beta_n \ell$ verses $\beta_n \ell$ and noting the values of $\beta_n \ell$ where the two curves intersect. These intersecting points satisfy equation 13. For $n > 5$ the eigenvalues for the free-pinned beam are approximately $\beta_n \ell = \frac{\pi}{4}(4n+1)$. When the values of the $\beta_n \ell$ have been determined, the natural frequencies of the beam may be calculated from equation 7, provided the size and material properties of the beam (i.e. E, I_z, ρ, ℓ and A) are known. Hence,

$$\omega_n^2 = \frac{EI_z}{\rho A} \frac{(\beta_n \ell)^4}{\ell^4} \tag{73}$$

Using the eigenvalues $\beta_n \ell$ for the free-pinned beam, the values of $\zeta_n(\beta_n \ell)$ may be determined by computing for each mode $\sin \beta_n \ell$ and $\sinh \beta_n \ell$, and substituting these values into equation 31. Note, however, that above the second mode the approximate value of ζ_n is:

$$\zeta_n(\beta_n \ell) = (-1)^n \frac{\sqrt{2}}{2}$$

The normal function $\frac{\Phi_n(\beta_n x)}{C_{1n}}$, or eigenfunction as it is often specified, defines the shape of the beam in each bending mode. Hence, it is a function of x and for the free-pinned beam it is given by equation 11. In the present calculations it is necessary to evaluate $\frac{\Phi_n(\beta_n x)}{C_{1n}}$ at stations $x/\ell = 0.2476$, and $x/\ell = 0.772$, the locations of the strain gage bridges.

Response data for the test beam were obtained for the five lowest horizontal bending modes; thus, it is necessary to know the values of $\beta_n \ell$, $\zeta_n(\beta_n \ell)$ and $\frac{\Phi_n(\beta_n x)}{C_{1n}}$ for n = 1, 2, 3, 4 and 5. The values of $\beta_n \ell$ and $\frac{\Phi_n(\beta_n x)}{C_{1n}}$ at the two strain gage locations are listed in beam tables [Reference (17)] for beams with various types of end constraints including the free-pinned beam. A summary of the beam parameters for the five lowest bending modes are listed in Table I, together

TABLE I: VALUES OF THE PARAMETERS FOR THE FIVE LOWEST BENDING MODES OF THE FREE-PINNED TEST BEAM.

n	f_n (cps) (Calculated)	ω_n (rad/sec)	$\beta_n \ell$	$2\zeta_n$	$\frac{\Phi_n(\beta_n x)}{C_{1n}}$ Sta. $x/\ell = 0.2476$	$\frac{\Phi_n(\beta_n x)}{C_{1n}}$ Sta. $x/\ell = 0.772$	$\Psi_n \times 10^4$ Sta. $x/\ell = 0.2476$	$\Psi_n \times 10^4$ Sta. $x/\ell = 0.772$
1	27.0	170	3.93	-1.46	0.64	1.12	-3.35	-6.2
2	87.5	550	7.07	1.42	1.33	-1.41	-12.9	-13.6
3	182	1140	10.2	-1.41	1.47	1.08	-20.6	-15.5
4	310	1950	13.35	1.41	0.85	-0.16	-15.0	-2.8
5	480	3020	16.5	-1.41	-0.14	-0.74	3.15	16.7

with the values of Ψ_n which is defined in equation 42a. Also included in Table I are the calculated values of the beam natural frequencies $\left[f_n = \frac{\omega_n}{2\pi}\right]$ as computed from equation 73.

The expansion of equation 42a, substituting numerical values from Table I for the five lowest bending modes at station $x/\ell = 0.772$, is

$$\frac{\epsilon_m(c)}{D_o} = -\frac{6.2\times10^{-4}}{\sqrt{\left[1-\frac{\omega_1^2}{\omega^2}\right]^2+\frac{\lambda_1^2}{\omega^2}}} - \frac{13.6\times10^{-4}}{\sqrt{\left[1-\frac{\omega_2^2}{\omega^2}\right]^2+\frac{\lambda_2^2}{\omega^2}}} - \frac{15.5\times10^{-4}}{\sqrt{\left[1-\frac{\omega_3^2}{\omega^2}\right]^2+\frac{\lambda_3^2}{\omega^2}}}$$

$$-\frac{2.8\times10^{-4}}{\sqrt{\left[1-\frac{\omega_4^2}{\omega^2}\right]^2+\frac{\lambda_4^2}{\omega^2}}} + \frac{16.7\times10^{-4}}{\sqrt{\left[1-\frac{\omega_5^2}{\omega^2}\right]^2+\frac{\lambda_5^2}{\omega^2}}} + \cdots\cdots \frac{\Psi_n\left(\frac{x}{\ell}=0.772\right)}{\sqrt{\left[1-\frac{\omega_n^2}{\omega^2}\right]^2+\frac{\lambda_n^2}{\omega^2}}} + \cdots \qquad (74)$$

Values of the damping coefficient λ_n as calculated from equation 74 and Table I are set forth in Table II. They are plotted as a function of the normal mode frequency in Figure VIII. The experimentally determined values of the beam natural frequencies also are included in Table II.

Table II: Average Experimental Values of the Damping Coefficients for the Five Lowest Beam Bending Modes.

Mode Number	f_n (cps) Experimental	ω_n (rad/sec) Experimental	λ_n @ $x/\ell = 0.2476$	λ_n @ $x/\ell = 0.772$
1	27.3	171	1.17	1.14
2	87.5	550	2.95	2.91
3	182	1140	8.43	8.96
4	310	1950	17.3	15.5
5	480	3020	32.9	31.2

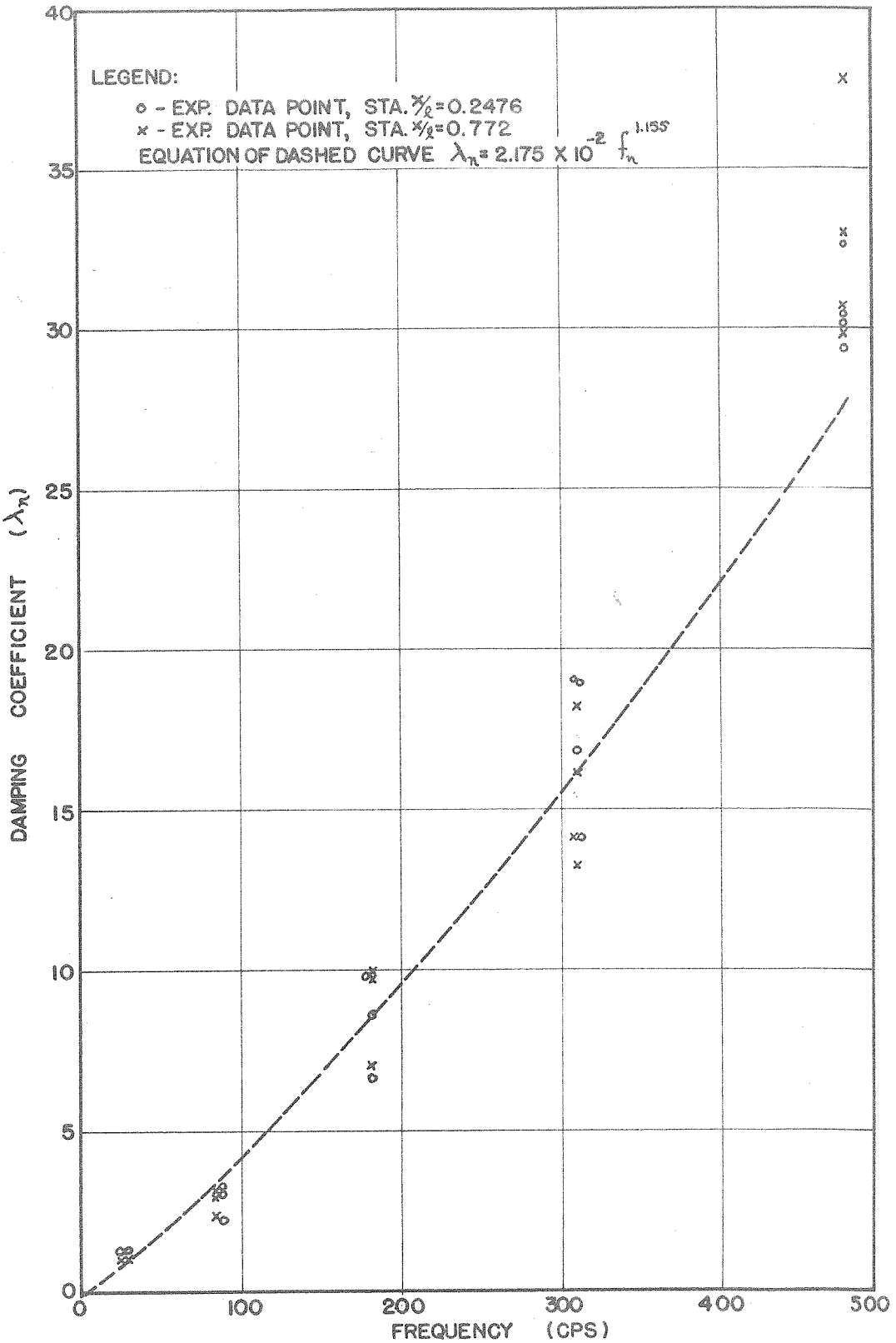

Figure VIII: Plot of the experimental damping coefficients (λ_n) versus the normal mode frequencies for the five lowest bending modes of the beam. The dashed line in this figure is the plot of an empirically defined equation that approximates the variation in beam damping as a function of the normal mode frequencies.

Based upon the variation of the damping in the five modes, as plotted in Figure VIII, and recognizing that λ_n is some function of the normal mode frequencies, we can define an empirical equation for the damping in the beam of the form:

$$\lambda_n = \mu \omega_n^{\alpha} \tag{75}$$

where the values of μ and α are determined by fitting a curve to the experimental data. Using a standard method of curve fitting in which by successive iterations the algebraic sum of the differences between the experimental data points and an assumed curve is minimized [see Reference (18)], the following values of μ and α were obtained

$$\mu = 2.62 \times 10^{-3} \tag{76a}$$

$$\alpha = 1.155 \tag{76b}$$

This curve is shown by dashed lines in Figure VIII.

It is common practice to define the damping in a single degree-of-freedom system as the fraction of critical damping, c/c_c. The same criterion may be used in a distributed mass system by considering the response in each normal mode to be analogous to that of a single degree-of-freedom system. Then the damping coefficient in equation 75 is related to the fraction of critical damping as follows:

$$\mu \omega_n^{\alpha} = 2(c/c_c)_n \omega_n$$

Solving for $(c/c_c)_n$:

$$(c/c_c)_n = \frac{\mu}{2} \omega_n^{\alpha-1} \tag{77}$$

Based upon the values $\mu = 2.62 \times 10^{-3}$ and $\alpha = 1.155$ the fraction of critical damping c/c_c is plotted in Figure IX as a function of the normal mode frequency f_n. In addition the values of c/c_c were

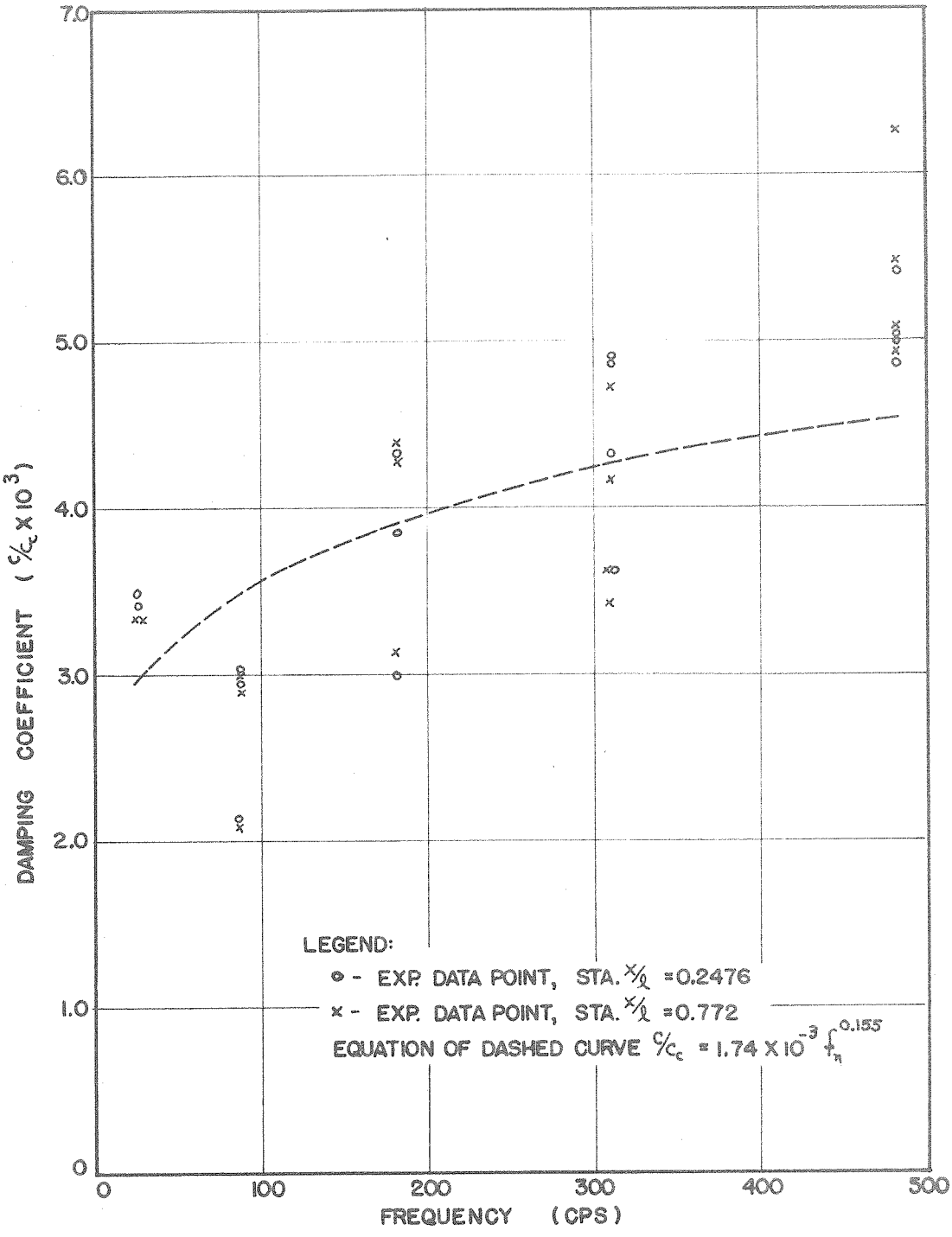

Figure IX: Plot of the fraction of critical damping (c/c_c) versus the normal mode frequencies for the five lowest bending modes of the free-pinned beam. The dashed curve is a plot of an empirically defined equation that approximates the damping in the beam.

TABLE III: SUMMARY OF TEST DATA

Test No.	Date of Test	Frequency (cps) Experimental	Input Displacement (in.)	Outer Fiber Strain (in./in.) x 10^4 Sta. x/ℓ = 0.2476	Outer Fiber Strain (in./in.) x 10^4 Sta. x/ℓ = 0.772	Calculated Values of λ_n	
						x/ℓ = 0.2476	x/ℓ = 0.772
1	4/12/60	27.3	0.0044	2.39	4.09	1.18	1.14
2	4/12/60	87.5	0.0010	2.17	2.31	3.30	3.25
3	4/12/60	182	0.0023	6.19	4.08	8.75	9.80
4	4/12/60	310	0.0012	1.85	0.38	19.0	18.3
5	4/12/60	480	0.00081	0.435	1.33	32.7	30.7
6	4/13/60	27.3	0.0035	1.87	3.26	1.16	1.14
7	4/13/60	87.5	0.0010	3.12	3.28	2.33	2.30
8	4/13/60	182	0.00077	1.84	1.33	9.84	10.0
9	4/13/60	310	0.0013	2.50	0.54	14.2	13.3
10	4/13/60	310	0.0023	3.97	0.89	16.9	14.2
11	4/13/60	480	0.00075	0.435	1.64	30.2	37.8
12	5/10/60	27.3	-	-	-	-	-
13	5/10/60	87.5	0.0021	4.70	4.93	3.23	3.20
14	5/10/60	182	0.0015	5.27	3.75	6.70	7.10
15	5/10/60	310	0.0030	4.57	1.02	19.1	16.2
16	5/10/60	480	0.00038	0.219	0.562	30.5	33.1
17	5/10/60	480	0.00031	0.186	0.525	29.4	29.8

calculated from the experimental values of the λ_n listed in Table III at stations $x/\ell = 0.2476$ and $x/\ell = 0.772$ using the equation

$$\lambda_n = 2(\%_c)\omega_n$$

These values are shown in Figure IX.

The ratio of the outer fiber strain amplitude as measured at station $x/\ell = 0.772$ to the displacement amplitude of the excitation is plotted in Figures X to XII as a function of the excitation frequency, for the first three bending modes of the beam. Data points for the three experimental curves were obtained by maintaining the outer fiber strain at a constant value of 0.863×10^{-4} in./in. while the excitation frequency and input amplitude were varied (see discussion in Testing Procedure on page 33). In addition, corresponding curves as calculated from equation 42 using the values of λ_n set forth in Table II are included in these figures. The calculated and experimental curves are normalized to the same values of response at resonance, and indicate the extent of agreement between theory and experiment at other frequencies.

D. DISCUSSION OF RESULTS

In the reduction of the experimental data, the damping coefficient (λ_n) was evaluated at each of the five lowest bending modes of the beam. By empirically fitting a curve to the experimental data points it was found that λ_n was proportional to the 1.155 power of the normal mode natural frequencies (ω_n). Some properties of the damping mechanism in the beam can be inferred by noting how λ_n varies with ω_n. For example, if λ_n is proportional to the first power of ω_n, then the

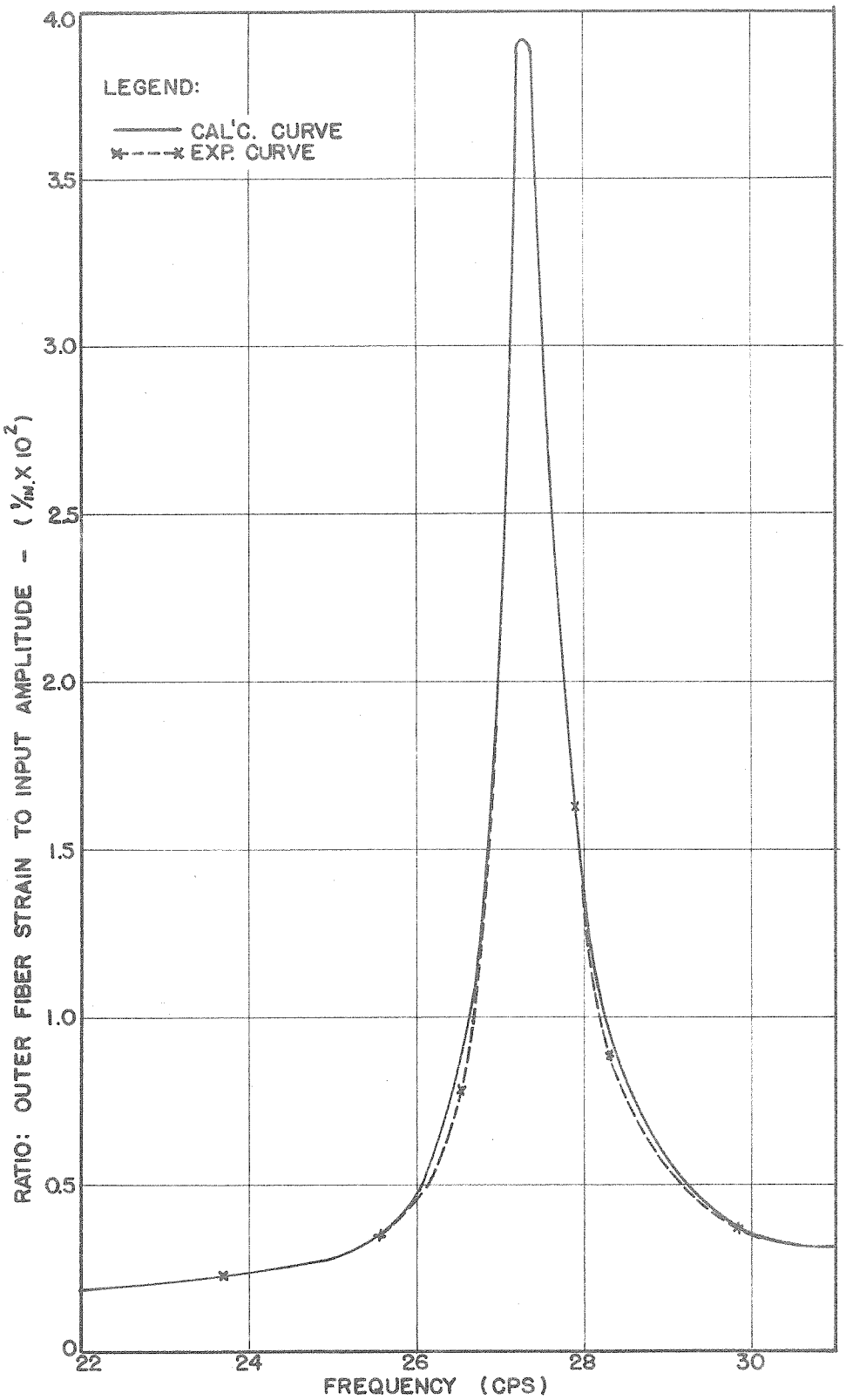

Figure X: Calculated and experimental response curves for the first bending mode at station $x/\ell = 0.772$.

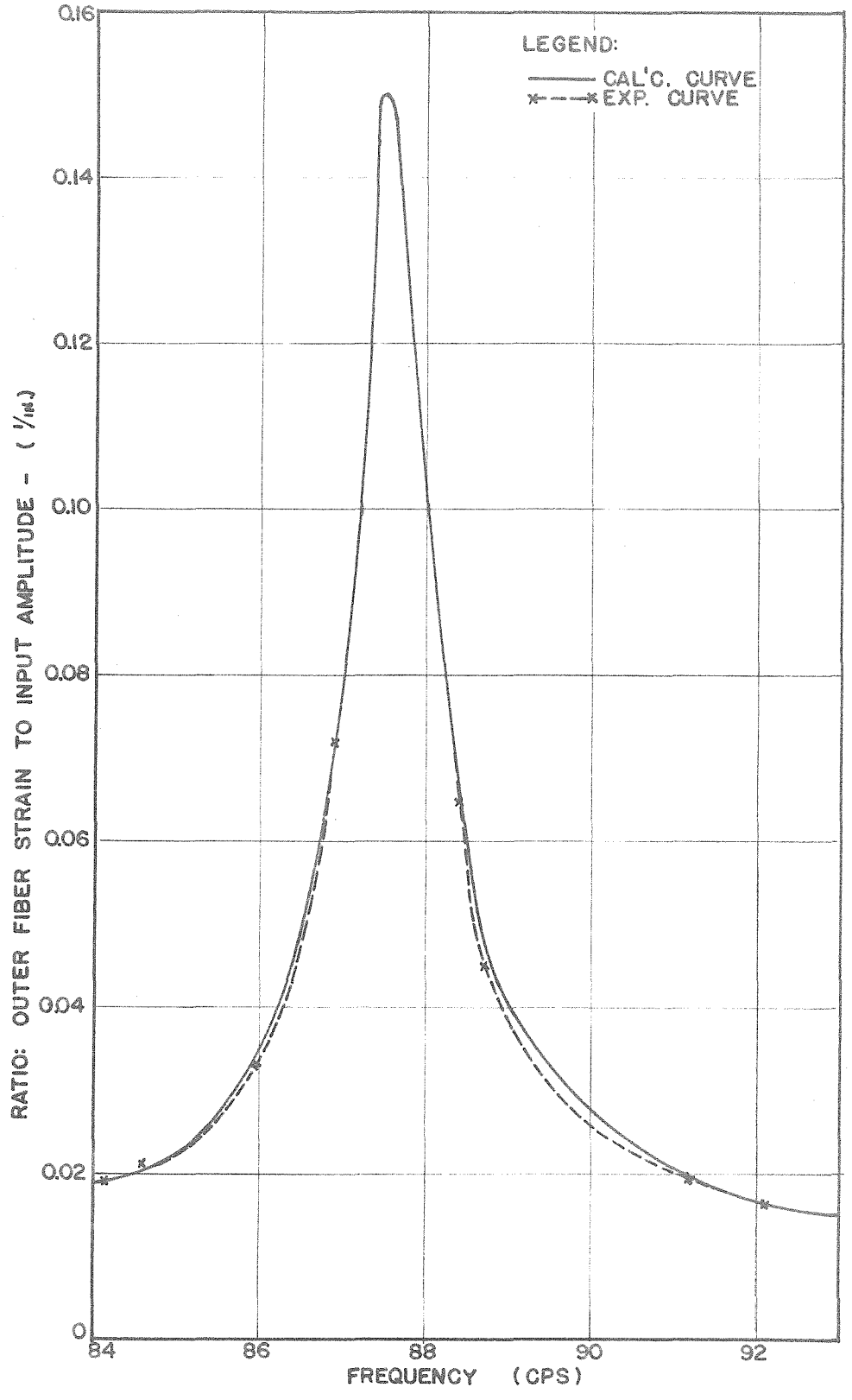

Figure XI: Calculated and experimental response curves for the second bending mode at station $x/\ell = 0.772$

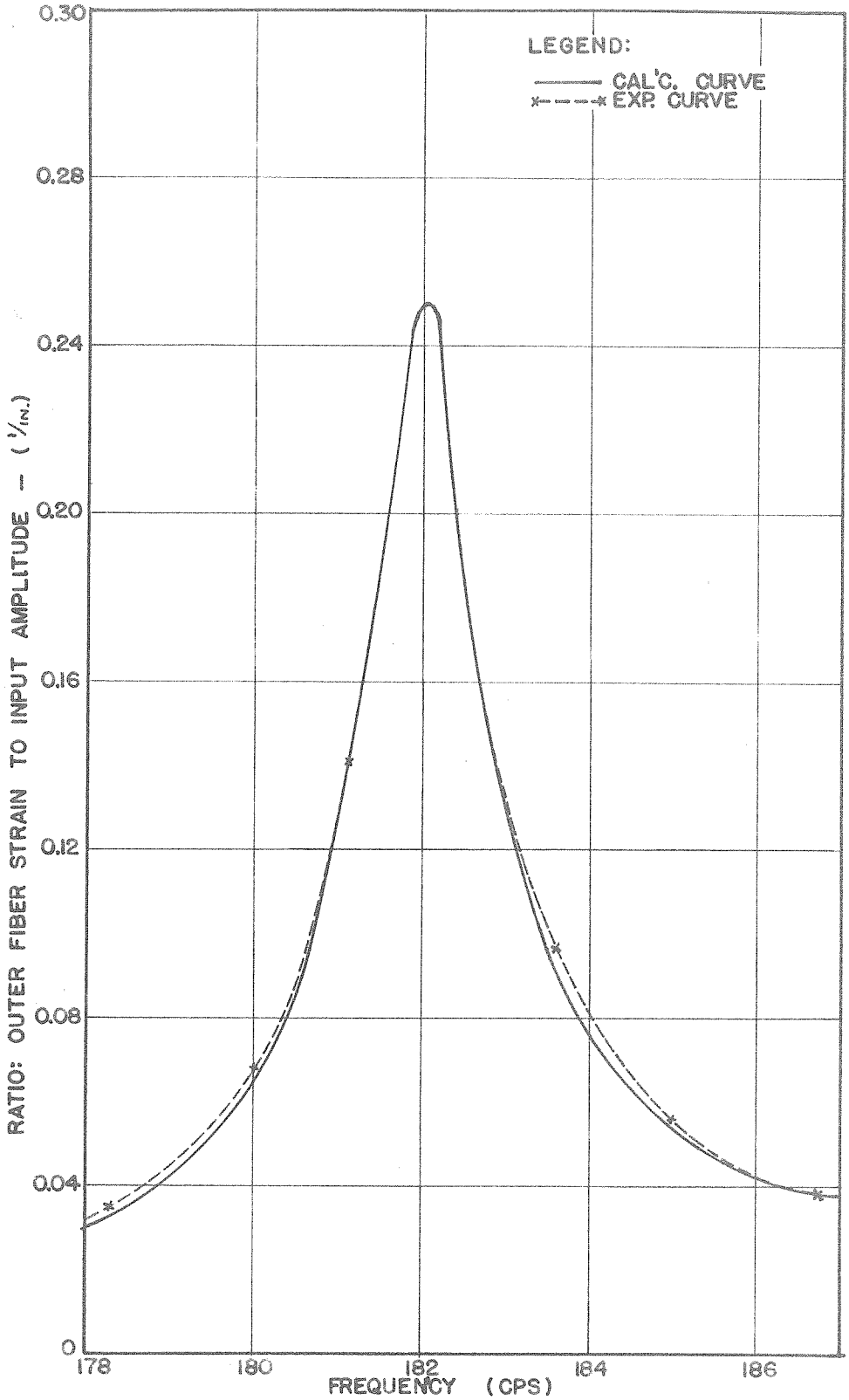

Figure XII: Calculated and experimental response curves for the third bending mode at station $x/\ell = 0.772$

beam responds in each normal mode in a manner similar to the response of a single degree-of-freedom system with viscous damping; i.e. the amplification factor Q has the same value at each resonant frequency. Unfortunately, as discussed by Mindlin, Stubner and Cooper (19), there is no known method of rigorously deriving a beam equation that includes a damping term whose coefficient is proportional to ω_n. The case when the damping coefficient varies with the second power of ω_n has been studied by Sezawa (20). He was able to derive the appropriate damping coefficient by selecting as the stress-strain law $\sigma = E(\epsilon + \nu \frac{\partial \epsilon}{\partial t})$ i.e. $H = \nu \frac{\partial}{\partial t}$ in equation 14. This type of damping is referred to as strain rate damping and is related to the hysteresis of the material. Therefore, based upon the experimentally determined power of ω_n of 1.155 and recognizing that the scatter of data is significant, we conclude that of the two damping models discussed above the low frequency damping mechanism in the free-pinned beam has characteristics more like viscous than strain rate damping.

The damping measurements obtained in this experiment are in agreement with those obtained by other experimenters. Germant (21) and Coleman (22) experimenting with thin steel tubes and built-up box beams, respectively, found that in the three lowest bending modes of these beams the amplification Q in each normal mode was constant. However, both experimenters obtained large scatter of data. More accurate data were obtained by Mindlin, Stubner and Cooper (19) in which they measured the damping in a simple cantilever beam excited transiently by a controlled half-sine wave pulse. They compared their experimental

results to various damping models and concluded that constant "Q" damping was most suitable in defining the damping in the cantilever beam during vibration of low frequency.

Experimentally determined response curves for the three lowest bending modes of the free-pinned beam were compared to calculated curves in Figures X to XII. Because the damping coefficients were calculated from measurements made at resonance, the calculated and experimental response curves have the same amplification at the resonant frequencies. In the immediate vicinity of resonance, only the calculated curves are shown since the frequency resolution in the experiment (see discussion in Testing Procedure on page 33) was not adequate to determine the exact shape of the curves. However, for frequencies away from resonance, general agreement between the two curves was obtained.

An original objective of this experiment was to determine the variation of damping in the beam with increase in outer fiber strain, for values of strain in the elastic region of the beam material. From the data in Table III it appears that the damping coefficient (λ_n) is unrelated to the strain level in the beam. However, small variations between λ_n and the outer fiber strain may have occurred, but due to inherent inaccuracies of the experiment such variations could not be detected. Results obtained by Lazan (23, 24) indicate that for mild steel the internal or hysteresis damping of the material is independent of the stress (or strain) below the fatigue limit of the material (29,000 psi). Whether this characteristic is true for a continuous system such as a beam has not been determined accurately.

To conclude, having evaluated an empirical relation for the damping as a function of the beam natural frequencies (equations 75 and 76), this relation can be used directly in the equation for response of the beam to random excitation (equations 57 and 59). If the value of the mean squared acceleration spectral density G is known, then the mean squared response of the beam can be evaluated.

APPENDIX A: CALCULATION OF THE CALIBRATION STRAIN VALUE

A calibration resistor (R_c) was built into the Wheatstone bridge circuit for strain gages. This resistor was connected between terminals 2 and 3 (see Figure XIII) with an on-off switch in series with it. Switching this resistor into the circuit caused a bridge unbalance which was measured in terms of a voltage Δe. The measured voltage represents a certain equivalent strain which must be calculated.

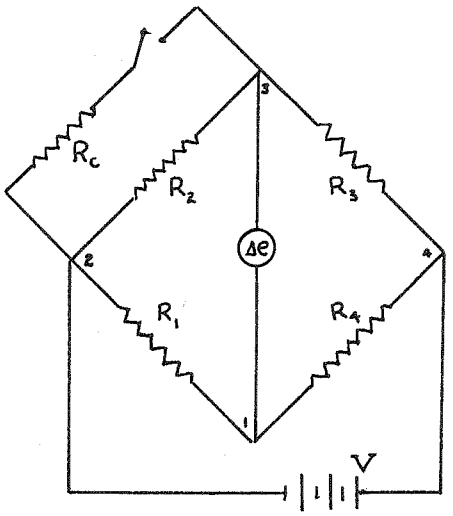

Figure XIII: Strain Gage Calibration Circuit

The total resistance R across terminals 2 and 3 is given by

$$\frac{1}{R} = \frac{1}{R_c} + \frac{1}{R_2} \tag{A-1}$$

Solving for R we obtain

$$R = \frac{R_c R_2}{R_c + R_2} \tag{A-2}$$

The change in resistance due to the addition of resistor R_c is

$$\Delta R_2 = R_2 - R = \frac{R_2^2}{R_c + R_2} \tag{A-3}$$

Hence

$$\frac{\Delta R_2}{R_2} = \frac{R_2}{R_c + R_2} \tag{A-4}$$

The basic equation for a four arm bridge is [Reference (25)]:

$$\frac{\Delta e}{V} = \frac{R_2 \Delta R_1}{(R_1 + R_2)^2} - \frac{R_1 \Delta R_2}{(R_1 + R_2)^2} + \frac{R_4 \Delta R_3}{(R_3 + R_4)^2} - \frac{R_3 \Delta R_4}{(R_3 + R_4)^2} \qquad (A-5)$$

With one active gage (R_2), the only resistance change is ΔR_2 and equation A-5 reduces to:

$$\frac{\Delta e}{V} = \frac{R_1 \Delta R_2}{(R_1 + R_2)^2} \qquad (A-6)$$

Let $R_1 = R_2$. Then

$$\frac{\Delta e}{V} = \frac{\Delta R_2}{4 R_2} \qquad (A-7)$$

Combining equations A-4 and A-7 leads to

$$\frac{\Delta e}{V} = \frac{R_2}{4(R_c + R_2)} \qquad (A-8)$$

The gage factor, which is a function of the strain gage material, is defined as follows:

$$K = \frac{\Delta R/R}{\epsilon} \qquad (A-9)$$

This equation indicates a constant relation between the change in resistance due to extension of the gage and the strain (ϵ) in the gage. We can solve equation A-9 for the strain with the aid of equation A-4 to obtain:

$$\epsilon_2 = \frac{R_2}{K(R_c + R_2)} \qquad (A-10)$$

Or from equation A-7 we can also write

$$\epsilon_2 = \frac{4 \Delta e}{K V} \qquad (A-11)$$

One calibration resistor that was used had a value of 44,000 ohms. The

resistance of the foil gages was 120 ohms and the gage factor was K = 2.01; thus the corresponding calibration strain was

$$\epsilon_2 = \frac{120}{2.01\,(44120)} = 1.36 \times 10^{-3} \ {}^{in.}/_{in.} \qquad \text{(A-12)}$$

APPENDIX B: EVALUATION OF THE INTEGRAL $\int_0^l x\,\Phi_n(\beta_n x)\,dx$

The integral

$$J = \int_0^l x\,\Phi_n(\beta_n x)\,dx$$

is to be evaluated for

$$\Phi_n(\beta_n x) = C_{1n}\left[\cos\beta_n x + \cosh\beta_n x - \alpha_n(\sin\beta_n x + \sinh\beta_n x)\right] \tag{B-1}$$

and

$$\alpha_n = \frac{\cos\beta_n l + \cosh\beta_n l}{\sin\beta_n l + \sinh\beta_n l} \tag{B-2}$$

Making the substitution $\beta_n x = z$, the integral equation reduces to the following:

$$J = \frac{C_{1n}}{\beta_n^2}\int_0^l\left[z\cos z + z\cosh z - \alpha_n(z\sin z + z\sinh z)\right]dz \tag{B-3}$$

Each of these integrals is listed in standard integral tables.

Evaluating the integrals at each limit results in the following:

$$J = \frac{2C_{1n}}{\beta_n}\left[\frac{l\sin\beta_n l\sinh\beta_n l + \frac{1}{\beta_n}(\sinh\beta_n l\cos\beta_n l - \cosh\beta_n l\sin\beta_n l)}{\sin\beta_n l + \sinh\beta_n l}\right] \tag{B-4}$$

As specified by equation 13, the frequency equation is

$$\tan\beta_n l - \tanh\beta_n l = 0$$

which may also be written in the form

$$\sin\beta_n l\cosh\beta_n l - \cos\beta_n l\sinh\beta_n l = 0 \tag{B-5}$$

Substitution of equation B-5 into equation B-4 yields

$$J = \frac{2C_{1n}l}{\beta_n}\,\frac{\sin\beta_n l\sinh\beta_n l}{\sin\beta_n l + \sinh\beta_n l} = \frac{2C_{1n}l\,S_n}{\beta_n} \tag{B-6}$$

Comparing equations B-6 and 30, we find that

$$x\int_0^l \Phi_n(\beta_n x)\,dx = l\int_0^l \Phi_n(\beta_n x)\,dx \tag{B-7}$$

LIST OF REFERENCES

(1) Rice, S. O., "Mathematical Analysis of Random Noise", Bell System Technical Journal, (1944), Vol. 23, pp. 282 - 332.

(2) Weiner, N., Estrapolation, Interpolation and Smoothing of Stationary Time Series, John Wiley and Sons, Inc., (1950), New York City, New York.

(3) Liepmann, H. W., "On the Application of Statistical Concepts to the Buffeting Problem", Journal of the Aeronautical Sciences, (1952), Vol. 19, No. 12, pp. 793 - 800 and 822.

(4) Miles, J. W., "On Structural Fatigue Under Random Loading", Journal of the Aeronautical Sciences, (1954), Vol. 21, No. 11, pp. 753 - 762.

(5) Lassiter, L. W., Hess, R. W. and Hubbard H. H., "An Experimental Study of the Response of Simple Panels to Intense Acoustic Loading", Journal of the Aeronautical Sciences, (1957), Vol. 24, No. 1, pp. 19 - 24 and 80.

(6) Thomson, W. T. and Barton, M. V., "The Response of Mechanical Systems to Random Excitation", Journal of Applied Mechanics, (1957), Vol. 24, No. 2, pp. 248 - 251.

LIST OF REFERENCES (CONTD.)

(7) Eringen, A. C., "Response of Beams and Plates to Random Loads", Journal of Applied Mechanics, (1957), Vol. 24, No. 1, pp. 46 - 52.

(8) Samuels, J. C. and Eringen, A. C., "Response of a Simply Supported Timoshenko Beam to a Purely Random Gaussian Process", Journal of Applied Mechanics, (1958), Vol. 25, No. 4, pp. 496 - 500.

(9) Weiner, N., Generalized Harmonic Analysis, Acta Mathematica, (1930) Vol. 55, 117 pp.

(10) Stumpf, H. J., Response of Mechanical Systems to Random Exciting Forces, U. S. Naval Ordnance Test Station, China Lake, Calif., (December 1959), NOTS TP 2365, NAVORD REPORT 7010, 231 pp.

(11) Ruzicka, J. E., editor, Structural Damping, The American Society of Mechanical Engineers, New York City, New York, (1959), 165 pp.

(12) Love, A. E. H., A Treatise on the Mathematical Theory of Elasticity, Dover Publications, New York City, New York, (1944), 643 pp.

(13) Timoshenko, S., Strength of Materials, part I, D. Van Nostrand Co., New York City, New York, third edition, (1955), 442 pp.

LIST OF REFERENCES (CONTD.)

(14) Kármán, T. V. and Biot, M. A., Mathematical Methods in Engineering, McGraw-Hill Book Co., New York City, New York, (1940), 505 pp.

(15) Crandall, S. H., editor, Random Vibration, Technology Press, Massachusetts Institute of Technology, Cambridge 39, Massachusetts, (1958), pp. 12 - 92.

(16) Grobner, W. and Hofreiter, N., Integraltafel, Springer-Verlag, Vienna, Austria, (1958), Vol. 1, 372 pp.

(17) Young, D. and Felgar, R. P., Tables of Characteristic Functions Representing Normal Modes of Vibration of a Beam, The University of Texas Publication, (July 1949), No. 4913, 31 pp.

(18) Worthing, A. G. and Geffner, J., Treatment of Experimental Data, John Wiley and Sons, Inc., New York City, New York, (1955), 344 pp.

(19) Mindlin, R. D., Stubner, F. W, and Cooper, H. L., "Response of Damped Elastic Systems to Transient Disturbances", Proceedings of the Society for Experimental Stress Analysis, Cambridge 39, Mass. (1948), Vol. 5, No. 2, pp. 69 - 87.

LIST OF REFERENCES (CONTD.)

(20) Sezawa, K., "On the Decay of Waves in Visco-Elastic Solid Bodies", Bulletin of the Earthquake Research Institute, Tokyo Imperial University, Vol. III, (1927), p. 50

(21) Gemant, A., "The Measurement of Solid Friction of Plastics", Journal of Applied Physics, (1940), Vol. 11, pp. 647 - 653.

(22) Coleman, R. P., Damping Formulas and Experimental Values of Damping in Flutter Models, National Advisory Committee for Aeronautics, (1940), TN 751, 27 pp.

(23) Lazan, B. J., "Effect of Damping Constants and Stress Distribution on the Resonance Response of Members", Journal of Applied Mechanics, Trans. ASME, (1953), Vol. 20, No. 2, pp. 201 - 209.

(24) Lazan, B. J., "A Study with New Equipment of the Effects of Fatigue Stress on the Damping Capacity and Elasticity of Mild Steel", Transactions of the American Society for Metals, (1950), Vol. 92, pp. 611 - 648.

(25) Perry, C. C. and Lissner, H. R., The Strain Gage Primer, McGraw-Hill Book Co., New York City, New York, (1955), 281 pp.